INTERNATIONAL JOURNAL OF ENERGY STUDIES

e-ISSN: 2717-7513 (ONLINE); homepage: https://dergipark.org.tr/en/pub/ijes

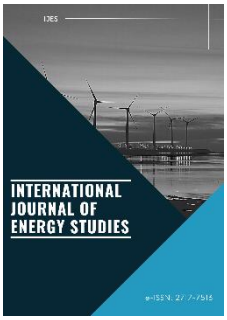

Research Article

Int J Energy Studies 2025; 10(1): 997-1042

DOI:10.58559/ijes.1573447

Received : 25 Oct 2024

Revised : 18 Feb 2025

Accepted : 24 Feb 2025

Life cycle assessment of photovoltaic systems of various sizes: An environmental and economic perspective on an educational building in a hot climate

Muhammed Enes Umcu[a], Ugur ACAR[b*], Önder KAŞKA[c]

[a]Osmaniye Korkut Ata University, Faculty of Engineering and Natural Sciences, Department of Mechanical Engineering, Osmaniye, Türkiye, ORCID: 0009-0002-1237-0431

[b]Osmaniye Korkut Ata University, Faculty of Engineering and Natural Sciences, Department of Mechanical Engineering, Osmaniye, Türkiye, ORCID: 0000-0002-6387-8641

[c]Osmaniye Korkut Ata University, Faculty of Engineering and Natural Sciences, Department of Mechanical Engineering, Osmaniye, Türkiye ORCID: 0000-0002-7284-2093

*(*Corresponding Author:uguracar@hotmail.com)*

Highlights

- Comprehensive yearly energy analysis was performed for an educational building.
- A realistic photovoltaic system has been modeled using various numbers.
- Simple payback period of 6.5 years was achieved.
- Carbon neutrality was reached within one year.

You can cite this article as: Umcu ME, Acar U, Kaşka Ö. Life cycle assessment of photovoltaic systems of various sizes: An environmental and economic perspective on an educational building in a hot climate. Int J Energy Studies 2025; 10(1): 997-1042.

ABSTRACT

The swift adoption of photovoltaic systems in buildings is driven by the need for sustainable energy solutions and decarbonization goals. This study assesses a faculty building's energy usage, potential energy yield, life cycle costs, and carbon emissions. Key factors such as building characteristics, operational schedules, and load profiles were analyzed using DesignBuilder. Photovoltaic system modeling with PVsyst explored various ground cover ratios (GCR). Life cycle cost analysis highlighted the economic advantages of photovoltaic systems, while carbon payback periods measured emission reductions. Results indicate that higher GCRs enhance energy production and revenue from grid sales. Performance ratio values varied between 77% and 79%, and the specific production rate ranged from 1630 to 1672 kWh/kWp. Although initial investment is high, increasing GCR reduces life cycle costs and shortens payback periods. Payback period was found to be 6.5 years, and the building achieves carbon neutrality within the first year. This methodology can be adapted for various building types and climates, supporting the broader goal of zero energy buildings and carbon emission reduction.

Keywords: Renewable energy, Life cycle carbon assessment, Life cycle cost analysis, Educational building

1. INTRODUCTION

The building sector accounts for approximately 20-40% of global energy consumption [1]. It is a major contributor to greenhouse gas emissions, which are responsible for global warming [2]. In 2021, the largest share in final energy consumption was taken by the industrial sector by 33.4% while households takes approximately 24% in Türkiye [3]. Energy efficiency considerations leads to 7,1 Mtep of cumulative savings between 2000-2015 for building sector in Türkiye [4]. In many countries, educational facilities and commercial buildings are prominent sources of concern when it comes to energy consumption, with educational buildings being particularly significant in terms of energy usage and carbon emissions compared to other types of buildings [5, 6]. Barbhuiyas indicated that educational buildings are responsible for a large amount of UK's non-industrial energy consumption [7].

Building energy models offer streamlined and effective prototypes for projecting future energy usage in buildings. These models can accurately calculate the energy requirements for heating, lighting, and cooling in buildings [8-10]. The literature survey showed that numerous studies concerning energy analysis of educational buildings have been performed. In this regard, cogeneration system with four patterns were evaluated to meet the load consumption of an educational building by Naserabad at al. [11]. The results of the study show that the highest energy and exergy efficiencies are 55,33% and 31%, respectively, which are related to the following thermal load. Zafaranchi and Sozer investigated various measures to enhance the energy efficiency of an educational building. They concluded that combined impact of the passive strategies results in an approximately 82% reduction in gas consumption and a 2% reduction in electric consumption [12]. Another study by Heracleous et al. suggests a design approach for retrofitting scenarios for educational buildings in the Mediterranean region [13]. Accordingly, insulation options for roof and walls were estimated to reduce primary energy demand 18% and 9% respectively, while windows provided a reduction of 3–4%. The sustainable retrofit options for two educational buildings in Iran were investigated using multi objective optimization method by Javid et al. [14]. The outcomes of the study show that utilizing reciprocating engine and exhaust-fired absorption chiller causes 17.79% and 20.8% of reduction in GWP of CO_2 equivalent for two considered buildings, respectively. Similar optimization studies concerning PV sizing resulted in more efficient solutions [15-17].

As a case study, the Mechanical Engineering Department building at Ain Shams University in Egypt, was modelled using Energyplus as a typical educational building to investigate various retrofitting strategies [18]. Results indicate that several building envelopes retrofitting strategies reduced the building energy consumption by more than 36% since it causes reduction in HVAC size by more than 65%. A study by Koo et al. aimed to propose an integrated approach for evaluating the impact of feed-in tariffs (FiT) on the life cycle economic performance of PV systems in educational facilities [19]. The research explored how China's zonal FiT policy influences economic performance through three utilization plans: No FiT plan, grid-connected utilization (GC) plan, and self-consumed utilization (SC) plan + grid-connected utilization (GC) plan. The study's results indicated that the break-even point for rooftop PV systems was 6.40 years for the SC + GC plan and 5.49 years for the GC plan. The goal of a study by Taghavifar and Zomorodian is to have a micro-hybrid energy system, consisting of solar and wind energy, installed in on-grid mode to allow the campus to sell any excess electricity generated back to the grid [20]. The findings revealed that a basic PV/grid system is suitable under low inflation conditions. However, as inflation rises, adding more equipment to the system becomes a more advantageous option. An increase in the number of wind turbines lowers the net present cost, while higher wind speeds contribute to a decrease in energy costs.

It was demonstrated by Ramon et al. that the minimum PV power required to achieve the ZEB standard is reduced in highly electrified buildings [21]. Meeting the ZEB condition can be accomplished by either decreasing energy imports or increasing renewable energy exports. In highly electrified buildings, installing a PV system addresses both requirements simultaneously. Omar et al. outline a strategy for converting a conventional educational building into a net-zero energy building [22]. For this retrofit methodology, an educational building in Egypt is chosen as a case study. Various strategies are employed to lower energy consumption, with the implementation of renewable energy systems achieving a renewable fraction of approximately 82%.

The potential of installing PV systems without battery storage on the rooftops of educational buildings with various roof tilt angles was studied by Khairi and Okajima.[23] Outcomes of the study finds that educational buildings with expansive rooftop areas and significant daytime energy demands are particularly well-suited for PV systems. Their electricity consumption patterns closely match solar production, allowing for more efficient use of clean energy. As a result, it is

noted that these buildings are more appropriate for installing solar PV systems compared to residential and office buildings. It is also stated that, due to the high energy consumption during the day, the need for energy storage is considered unnecessary for educational buildings. Another study conducted by Park et al. aimed to identify the best strategy for deploying PV systems to achieve the national carbon emissions reduction target for educational facilities in Korea [24]. The findings revealed that the mono-Si PV system is the most efficient option for these facilities. A study by Gbadamosi et al. assesses the technical, economic, and environmental advantages of utilizing renewable energy sources for supplying electricity to large buildings in an educational institution [25]. They found that a combination of grid and PV systems offers an optimal solution that effectively meets the load demand with increased renewable energy integration. This approach reduces energy costs by 45% and lowers CO_2 emissions by 32.09%. The economic and energy performance impacts of integrating retrofit measures with renewable energy strategies for a university building in Recife, Brazil, are examined by Munguba et al. [26]. The results show that combining thermal modeling, economic analysis, and optimization identifies synergistic retrofit measures and photovoltaic sizing configurations that reduce energy consumption by over 45 MWh per year and improve the net present value by more than $170,000 compared to baseline performance, all without additional investment. Another analysis of the techno-economic feasibility of using PV systems to achieve net-zero energy in academic buildings was conducted by Kabir et al.[27]. The findings indicate that optimally sized PV systems can produce a net positive energy balance for universities, high schools, and primary schools. Economic viability was evaluated, revealing that each scenario achieved positive net present value and profitability index values exceeding 1. The decarbonization analysis also demonstrated notable reductions in CO_2 emissions across all three types of buildings.

Leichter and Piccardo conducted a review of 44 articles to identify trends in the methodological approaches of comparative studies focused on renovation and reconstruction scenarios [28]. The review highlights that the most extensively researched aspect is building scale, with life cycle assessment being the most commonly utilized method. While cost analysis is, frequently employed, social factors are often overlooked. Another study by Hemmati and Ebel brought attention to the growing use of artificial intelligence in evaluating sustainability [29].

The integration of a life cycle approach and occupant thermal comfort into the energy efficiency design of school buildings is aimed to be explored by the study conducted by Moazzen et al.[30].

The primary aim is on evaluating the energy use and environmental impacts of various building envelope alternatives across three different climatic regions in Türkiye. In both temperate and cold climates, the proposed strategies can enhance comfort conditions. The proportion of embodied energy and carbon at the net-zero energy building level can exceed 80 percent, whereas it remains below 15 percent at the cost-optimal level.

Aktas and Ozenc investigated the feasibility of a rooftop PV system for a college building in Siirt, Türkiye [31]. The PV system was analyzed using PVsyst software. However, the building's energy loads were determined based on the installed capacity of devices and approximate daily usage times, rather than through detailed hourly simulations. The results showed that the system achieved a performance ratio of 84%, with total carbon emission savings of 6852 tons of CO_2. Özcan et al. examined the feasibility integration of PV system into residential building with three different types of batteries in Antalya and İstanbul [32]. The researchers used Beopt software for energy modeling and Homer software for PV system modeling. Payback periods are calculated between 8.9 and 11.7 years. A CO_2 emission reduction of 238 kg/year and 928 kg/year was achieved using second-life Li-ion batteries.

Sevik conducted an analysis of a grid-connected PV-trigeneration-hydrogen production system using Helioscope software at Hitit University Campus, Türkiye [33]. The total CO_2 reduction achieved by the proposed system over the project's lifetime was estimated to range from 1546 to 2272 tons of CO_2 equivalent emissions, varying by scenario. Additionally, a payback period of 5.5 years, a performance ratio of 78.7%, and a specific production of 1,313.7 kWh/kWp were calculated, concluding that electricity generation with PV is the most cost-effective system. Alıç conducted a techno-economic analysis of rooftop and sun-tracking PV systems installed on the campus of Kahramanmaraş Sütçü İmam University, incorporating various energy storage and management systems [34]. Environmental aspects have not been considered in the solutions. The payback period for the 5kWp rooftop PV system without energy storage was found to be 8.38 years. Economic evaluation has shown that rooftop PV systems are more cost-effective than sun-tracking PV systems.

Bilir and Yildirim, evaluated the feasibility of installing 2 different numbers of on-grid PV systems on a school building in Izmir, Türkiye, demonstrating that the systems could meet or exceed annual energy demands (110–162% coverage) with a 7.6–7.9 year payback period while reducing

greenhouse gas emissions [35]. Dal and Ashrafian evaluates 111 building retrofit packages for a school building in Istanbul, Türkiye [36]. PV panel solutions with three different sizes are among the solution scenarios. Findings indicated that combining enhanced insulation, triple low-E glazing, LED lighting, and renewable energy systems (30 kW PV panels with heat pumps) reduces total primary energy consumption from 93.05 kWh/m² to 3.35 kWh/m², offering a pathway to near-zero energy performance.

Atmaca and Atmaca conducted a detailed study concerning life cycle carbon assessment of two residential buildings including all building materials used in construction phase in Gaziantep, Türkiye [37]. Throughout the lifetime of the buildings, the operational phase was the major factor, contributing to 86–93% of the total CO_2 emissions. Authors also investigated carbon footprint of another residential building as a case study and stated that 1513 kg.CO_2e per year may be prevented by PV panels by using available roof area [38].

Kayaçetin and Hozatlı investigated the environmental impact of improved building envelope and technical systems for residential and office buildings in Turkiye [39]. Life cycle carbon assessments, which include operational carbon emissions, have been performed using projected grid mix forecasts. The findings revealed that operational carbon emissions ranged from 53% to 90%, influenced by the type of building. Kınay et al. highlighted that current insulation standards based on climatic zones are inadequate for achieving carbon-neutral buildings in Türkiye [40].Kayaçetin and Tanyer analyzed the embodied carbon impact of neighborhood-scale developments by examining three large-scale housing projects developed by Türkiye's Housing Development Administration (TOKI) [41]. Their research highlighted that buildings account for the largest share of embodied carbon emissions in such community-level developments.

To the best of our knowledge, no comprehensive studies in the literature have simultaneously addressed both the economic and environmental aspects of rooftop PV system feasibility, following a detailed energy analysis, in educational buildings in Türkiye. While all the studies mentioned above have made valuable contributions to the literature, none have examined key parameters such as ground cover ratios, performance ratio, solar factor, life cycle costs, payback periods, and carbon payback time simultaneously together within the context of the net zero energy building concept, as a case study of a real educational building. In this article, an in-depth analysis has been conducted on a faculty building's energy consumption, potential energy generation from

solar PV systems, life cycle costs, and life cycle carbon emissions. All details about the building description, climate data, thermal model, schedules, lighting, plug loads have been presented as crucial for accurate energy modeling. The detailed modeling of the PV system using PVsyst software has been established, considering various ground cover ratios (GCRs). Performance indicators such as grid interaction index, performance ratio, solar factor, and energy use intensity have been calculated for all scenarios considered in this study. A comprehensive life cycle cost analysis has been conducted, and the simple payback period has been calculated for economic benefit assessment. For the environmental impact analysis, the life cycle assessment method has been employed to evaluate carbon emissions, and carbon payback periods have been calculated. The applied method can be adapted for different building types and climates, to increase PV system usage and achieving zero energy buildings within a carbon reduction framework.

2. MATERIAL AND METHOD

Evaluating building energy consumption is a complex process. To perform an accurate energy analysis, factors such as envelope characteristics, weather conditions, internal gains, operating schedules, and temperature set points must be determined precisely. Changes in any of these parameters can affect the energy analysis. All these parameters should accurately represent the real conditions of the building. Researchers use a variety of energy modeling software for this purpose. EnergyPlus is one of the most widely used whole-building energy simulation programs, capable of modeling energy consumption for heating, cooling, ventilation, lighting, and plug loads in buildings and BESTEST compliance for realistic simulations [42]. DesignBuilder, which is a popular commercial, third-party modeler and interface for the EnergyPlus simulation engine, was used in this study since the core EnergyPlus graphical interface is not very user-friendly.

2.1. Building description

The building of the Osmaniye Korkut Ata University Engineering Faculty, located in the central district of Osmaniye, Türkiye, is the subject of this study. It is a prominent educational institution offering engineering education across various disciplines. Like many educational institutions, the engineering faculty building, which is actively used by students and researchers, is responsible for a significant portion of the campus's overall energy consumption. The building faces 24 degrees to the north, as shown in Figure 1. This figure provides a rendered view of the building exported from DesignBuilder, visualizing the sun's path throughout the year for the studied location (Lat: 37.038003, Long: 36.223714).

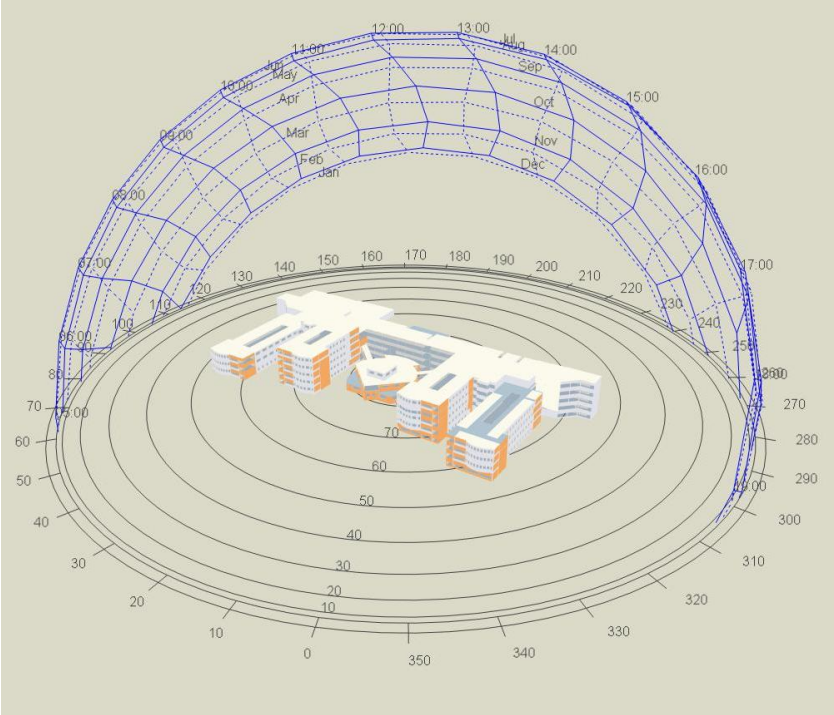

Figure 1. Sun-path diagram

The building has a total of five floors, with a floor area of 10,130.00 m² and a gross area of 38,230.51 m². The ceiling height is 4.2 meters. Constructed in 2014, the building was designed to comply with thermal insulation requirements for buildings in Türkiye [43]. An aerial view and a 3D model of the building are provided in Figure 2 and Figure 3.

Figure 2. Aerial view of the building

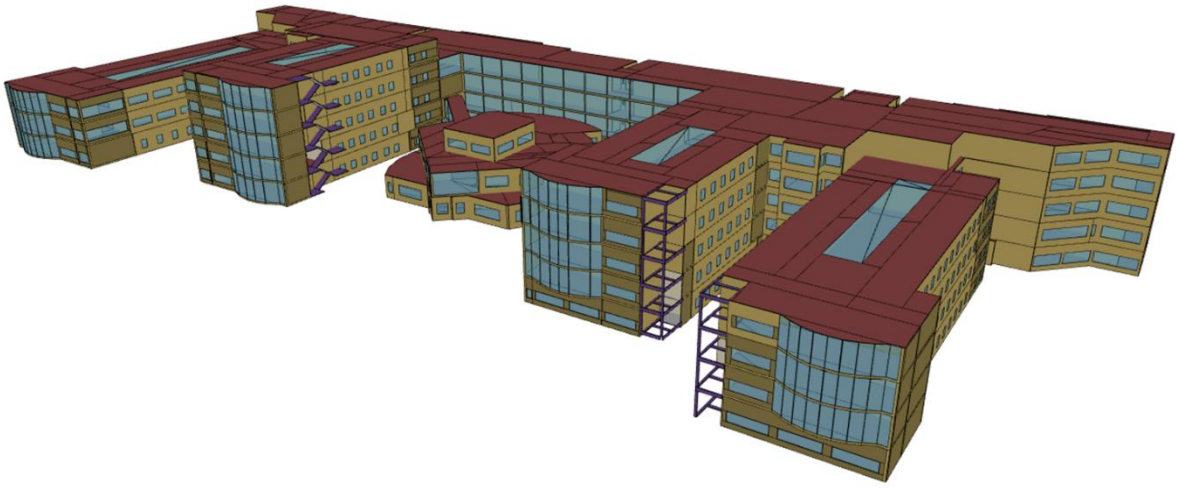

Figure 3. 3D model of the building

Floor plans were imported into the DesignBuilder software from the architectural plans. Floors were then created based on these 2D plans. Each office, classroom, workshop, and other room types were modeled separately. These separate volumes are referred to as zones. Rooms of the same type that share adjacent walls, such as classrooms, are combined into a single zone since all thermostat settings, occupancy schedules, and occupant densities are the same. The second-floor plan of the building is shown in Figure 4.

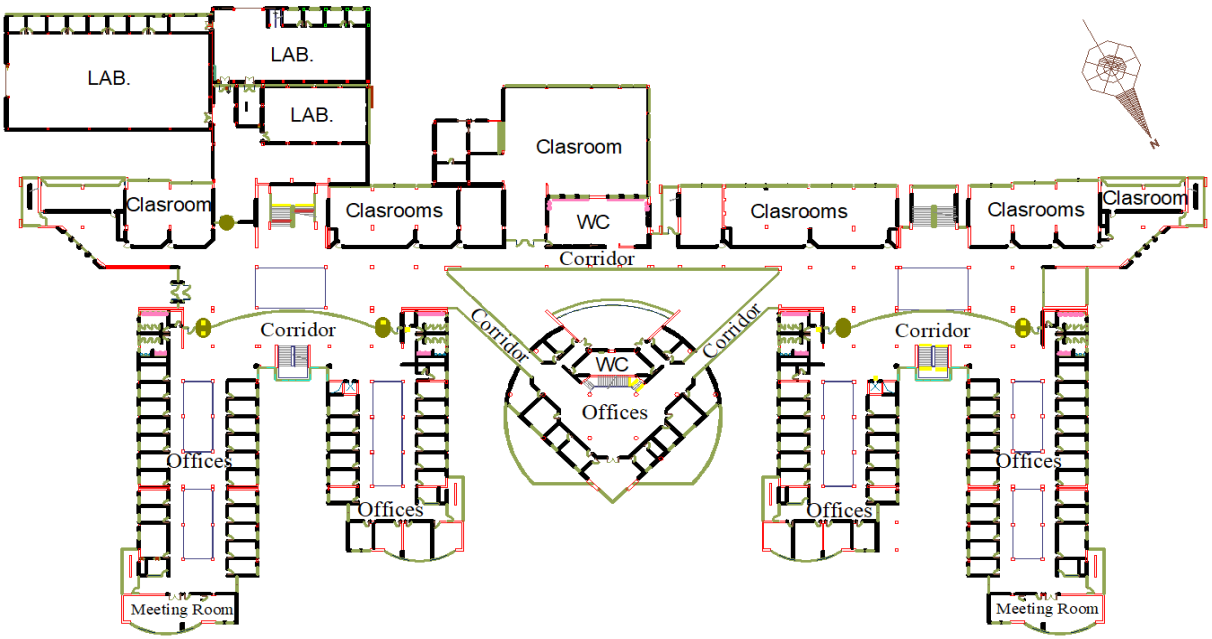

Figure 4. Second floor plan

The building envelope has the greatest influence on the energy exchange between buildings and their surroundings [44]. It accounts for a significant proportion of the total energy consumption of the buildings [45]. Different design choices for the building envelope can have varying energy consequences [46-48].

The largest portion of the building envelope under investigation consists of exterior walls. There are two types of exterior walls in the building. The first type is a structural component heavily composed of reinforced concrete, while the second type of exterior wall and the interior walls do not include reinforced concrete. All exterior walls are insulated with extruded polystyrene panels. The roof is a flat concrete type, covered with elastomeric bitumen for water insulation. All related information, such as wall elements and material thickness, was obtained from architectural plans, while some unknown values, such as specific heat, were estimated based on experience and knowledge. The considered U-values of the envelope components for the energy analysis are given in Table 1.

Table 1. U-values

Component	**U-value (W/m^2-K)**
Exterior Wall 1	0.55
Exterior Wall 2	0.50
Roof	0.45
Ground Floor	0.60
Windows	2.645

Windows are identified as double-glazing with aluminum frames according to field inspections. The glazing thickness is 6 mm, with a 13 mm air gap between the layers. The window U-value is 2.645 $W/m^2 \cdot K$, while the solar heat gain coefficient (SHGC) and visible transmittance are 0.7 and 0.78, respectively. According to the architectural plans, the windows on the southern façade have a window-to-wall ratio (WWR) of 42%, while the windows in the corridors on the northern façade have a WWR of 100%. All other windows are sized based on architectural drawings and verified through on-site building inspections.

2.2. Climate data

Building energy consumption is influenced by weather conditions. A Typical Meteorological Year (TMY) dataset was used to model these conditions. It provides a representative set of weather

parameters for the entire lifespan of the building. Acar et al. compared the TMY data offered by the Meteonorm firm with the data provided by Crawley and Lawrie [49, 50]. The results showed that these two weather datasets are remarkably similar, so this study used the TMY data provided by Crawley and Lawrie.

Heating degree days (HDD) and cooling degree days (CDD) for Osmaniye provinces were calculated using data from the TMY file with a base temperature of 18°C. Climate region according to Köppen-Geiger [51] and the Turkish Standard [52] are given in Table 2. Monthly variation of global horizontal radiation, horizontal diffuse radiation and average dry bulb temperature is shown in Figure 5. The Global horizontal radiation value at 1789 kWh/m² per year exceeds the national average for Türkiye, which is 1527 kWh/m². This location has a Mediterranean climate, marked by hot, dry summers and mild, wet winters. The average dry bulb temperature is 18.8°C, with a maximum recorded temperature of 45.6°C in 2023 and a minimum of -8.5°C in 1989.

Table 2. Climate characteristics

Province	Climate Zone		HDD	CDD
	Köppen-Geiger	TS825	(T_b=18°C)	
Osmaniye	Csa	1	986	1399

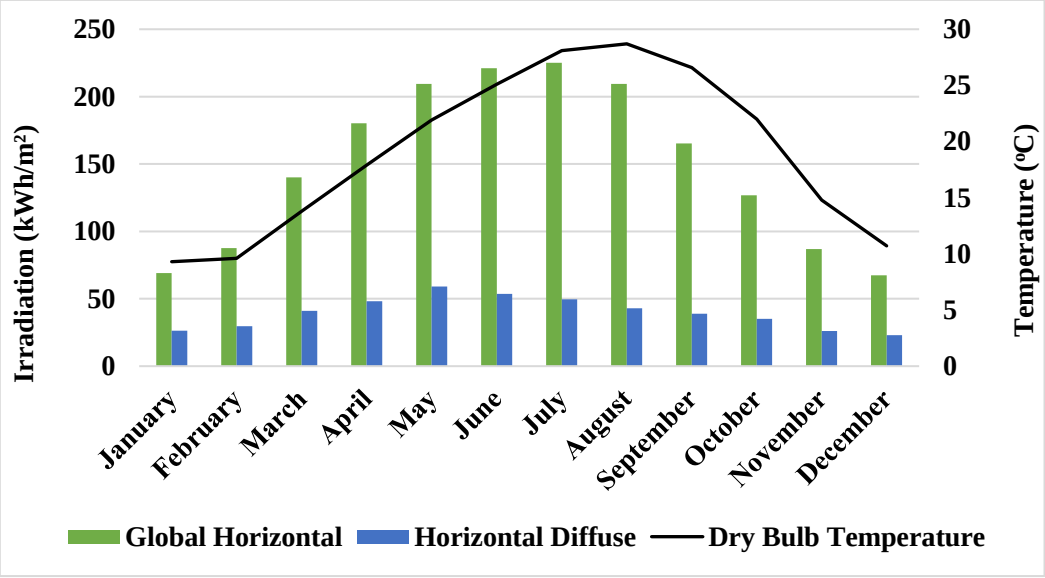

Figure 5. Monthly climatic values

2.3. Thermal model

EnergyPlus employs the ASHRAE Heat Balance Method, which relies on a series of heat balance equations for zone air as well as each exterior and interior surface surfaces [53]. In essence, the heat balance method requires that the algebraic sum of convection, radiation, and absorbed solar heat gain at the exterior surface equals the conduction into the wall [54]. Subsequently, the zone load is determined based on the conductive heat flux through the external wall element. To capture the dynamic nature of energy consumption, the simulation employed a time step of 30 minutes.

The building utilizes a variable refrigerant flow (VRF) central air conditioning system for both heating and cooling. All ceiling type indoor units are connected to an outdoor unit. Expansion valves in indoor units control the amount of refrigerant based on cooling or heating demand of the zone. All indoor and outdoor units are sized based on a yearly energy analysis using the design day sizing method, with a safety factor of 15%. The coefficient of performance (COP) for heating and cooling is taken as 3.4 and 3.3, respectively. Design conditions for the nearest meteorological station, based on the annual frequency of occurrence of 99.6% for heating and 0.4% for cooling, are provided in Table 3.

Table 3. Design Conditions

Design Season	DB Temperature (ºC)	Daily Temperature Range (ΔT)	Mean Coincident WB (ºC)	Wind Speed (m/s)
Summer	36.80	9.90	22.20	0.0
Winter	1.10	0.00	1.10	9.1

To ensure occupant comfort throughout the year, the thermal zones were designed to maintain temperatures within the ranges recommended by ASHRAE 55 Standard [55]. This standard suggests a temperature range of 22-26°C for summer and 20-23°C for winter. In line with these guidelines, the thermal zone temperatures were set at 22°C for heating and 24°C for cooling. The zones are heated or cooled depending on occupancy schedule.

Infiltration, also known as air leakage, refers to uncontrolled natural ventilation. This phenomenon typically occurs through gaps or cracks in the building envelope, as well as around inadequately sealed windows and doors [56]. The infiltration rate is defined as 0.5 air change per hour (ACH) which is used for buildings with good airtightness and well-framed windows [57].

2.4. Schedules

Schedules play a significant role in energy calculations, as highlighted by Delzendeh et al.[58], by specifying the days and hours during which a particular area will be used. Two occupancy schedules, namely 'Classroom Schedule' and 'Office Schedule,' have been established based on field inspections. Both schedules maintain the same set temperatures. The Classroom Schedule applies to weekdays from September 19th to June 15th, with usage hours from 9:00 AM to 4:00 PM. Weekends and the period from January 22nd to February 15th (semester break) are excluded. The Office Schedule applies to weekdays throughout the year, with usage hours from 8:00 AM to 5:00 PM. Weekends are off for offices. Notably, office occupancy density experiences a significant reduction from 100% to 40% during the summer period (June 15th to September 19th) due to annual leaves. Laboratories follow the Classroom Schedule in terms of usage hours but have a different people density per unit area. Occupancy schedules for corridors, workshops, and storage zones mirror the Office Schedule; however, these zones will have a significantly lower occupant density compared to offices, especially corridors. Two distinct activity levels are considered: 108 watts per person for seated activities and 126 watts per person for standing activities. Seated activities apply to those in classrooms, offices, and laboratories, whereas standing activities apply to corridors, workshops, and storage zones. Details on occupancy schedules and related densities are provided in Table 4.

Table 4. Schedules and occupancy densities

Zone	Operating Days	Operating Hours	Occupancy Density (people/m^2)	Hourly Fractions of Occupancy / Equipment
Office	Weekdays (Occupant density reduced 40% from June 15th to September 19th)	8:00 am to 5:00 pm	0.1030	07.00–08.00 = 0.25; 08.00–12.00 = 1.00; 12.00–13.00 = 0.25; 13.00–17.00 = 1.00; 17.00–18.00 = 0.25; 18.00–07.00 = 0
Classroom	Weekdays between September 19th and June 15th (Except from January 22nd to February 15th)	9:00 am to 4:00 pm	0.2034	08.00–09.00 = 0.25; 09.00–12.00 = 1.00; 12.00–14.00 = 0.50; 14.00–16.00 = 1.00; 16.00–17.00 = 0.25; 17.00–07.00 = 0

Laboratory		9:00 am to 4:00 pm	0.2313	10.00–12.00 = 1; 12.00–13.00 = 0; 13.00–15.00 = 1
Corridor		8:00 am to 5:00 pm	0.1065	07.00–12.00 = 0.25; 12.00–13.00 = 0.90; 13.00–18.00 = 0.25; 18.00–07.00 = 0
WC	Weekdays	8:00 am to 5:00 pm	0.1065	07.00–12.00 = 0.25; 12.00–13.00 = 0.90; 13.00–18.00 = 0.25; 18.00–07.00 = 0
Meeting Room		8:00 am to 5:00 pm	0.1030	10.00–12.00 = 1; 12.00–13.00 = 0; 13.00–15.00 = 1

2.5. Lighting

The lighting design for the building was verified following an on-site inspection. Tubular Fluorescent lamps were identified for illumination. When defining lighting parameters in the energy model, it is essential to express the lighting in the zone using units of W/m², known as Lighting Power Density (LPD), and to specify the type of illumination, such as Recessed or Suspended. If the lighting control is not explicitly defined, EnergyPlus will default to a 100% on status for all defined schedule values. Therefore, a lighting control strategy was implemented in the model. The selected lighting control strategy is based on linear control, where the lighting intensity is adjusted according to zone illumination levels in lux. If the zone's illumination value falls below the set lux level, the lighting control will increase the lighting linearly to maintain the desired illumination level.

Various standards and guidelines suggest that learning spaces should have an illuminance level ranging from 300 lux to 500 lux [59]. For educational buildings, a minimum illuminance level of 400 lux defined by IESNA [60]. The illumination level is set for 500 lux for every zone except corridors. Considered illumination levels and lighting power densities are given in Table 5.

Table 5. Lighting characteristics

Zone	Illumination Level (lux)	Lighting Power Density (W/m^2)
Office	500	9
Classroom	500	12.6

Laboratory	500	12.6
Corridor	100	0.62
WC	100	0.62
Meeting Room	500	9

2.6. Plug loads

Plug loads refer to all electric loads in a building except those associated with main systems for heating, cooling, ventilation, and lighting [61]. Plug loads can account for a significant portion of the energy used in commercial buildings [62], and it is anticipated that this percentage will experience a projected increase of 40% over the next 20 years [63, 64]. As a result, plug loads have emerged as one of the rapidly expanding load categories [65]. Hence, the modeling of plug loads gains significant importance. The plug loads for the building were determined through both on-site inspection and ASHRAE 90.1 Standard. The considered plug load values for each zone type can be seen in Table 6. Plug loads are associated with the on occupancy schedules.

Table 6. Plug Load Densities

Zone	**Plug Load (W/m^2)**
Office	11.99
Classroom	4.74
Laboratory	27.81
Corridor	0
WC	0
Meeting Room	4.74

2.7. Photovoltaic panels

PVsyst software was utilized to create a detailed model of the PV system and simulate its performance. This software incorporates numerous factors that influence energy generation, such as solar radiation data, panel characteristics, and system losses. It employs the one-diode model which is widely used for realistic calculations [66]. The primary equation that describes current supplied by the module, *I*, based on the one-diode model under a specific set of reference conditions (1000 W/m^2, 25°C, AM=1.5) is expressed as;

$$I = I_{ph} - I_0 \left[exp\left(\frac{q(V + R_s I)}{N_{cs} k \gamma T_c} \right) - 1 \right] - \frac{V + R_s I}{R_{sh}}, \quad (1)$$

where I_{ph} represents photocurrent, I_0 represents the diode's saturation current, and V is the voltage across the module's terminals. R_s and R_{sh} correspond to the series and parallel resistances, respectively. Certain constants, including the electron charge (q), Boltzmann's constant (k), and the diode quality factor (γ), are used in Equation 1. T_c and N_{cs} denote the effective temperature of the cells and the number of cells connected in series, respectively.

The one-diode model assumes that the photocurrent, I_{ph}, is directly proportional to the irradiance, with a minor temperature dependence that increases linearly in relation to the temperature coefficient of short-circuit current parameter, μ_{ISC}, allowing I_{ph} to be calculated for any given conditions as follows:

$$I_{ph} = \frac{G}{G_{ref}} \left[I_{ph,ref} + \mu_{ISC} \left(T_c - T_{ref} \right) \right], \quad (2)$$

with G and G_{ref} represents the effective and reference irradiance (W/m²), respectively. Monocrystalline PV panel characteristics are given in Table 7.

Table 7. Solar panel characteristics

Property	**Value**
Nominal Power	300 W
Dimensions	1648x995mm
Number of Cells	60
Module Efficiency	18.30%
V_{mp}	33.08 V
I_{mp}	9.08 A
V_{oc}	39.06 V
I_{sc}	10.03 A
Temperature Coefficient of I_{sc}	0.048%/°C
Temperature Coefficient of V_{oc}	-0.28%/°C
Temperature Coefficient of P_{max}	-0.37%/°C

DC-AC inverter of 125kW with an efficiency of 97% was used. The number of inverters used in the system determined by array configuration and design voltage and ampere values of inverter. PV panels were installed only on the roof. The panels were oriented with a south-facing azimuth angle of 0 degrees for optimal sun exposure. A tilt angle of 35°, as suggested by Acar et al., was chosen to maximize energy generation throughout the year [67]. To ensure a seamless and accurate evaluation of the building's energy performance with integrated solar power, both the energy modeling and the PV system analysis utilized the same weather data. This consistent approach creates a reliable framework for assessing the building's energy consumption and the potential benefits of the PV system. Furthermore, the PV analysis integrates the hourly consumption data obtained from the energy calculations, allowing the PV model to understand the building's specific energy demand patterns throughout the year. Degradation rate of 0.7% was assumed [68].

PV arrays cover some portion of installed area whether it is on the roof or on the ground. In order to define how much area covered by PV panels, ground cover ratio (GCR) is used. It is an important parameter in designing solar systems, as it directly affects the system's efficiency. A schematic representation of array installation on roof is depicted in Figure 6. GCR is essentially the ratio of module area to land area [69]. It is calculated according to Equation 3.

$$GCR = \frac{L}{R} \tag{3}$$

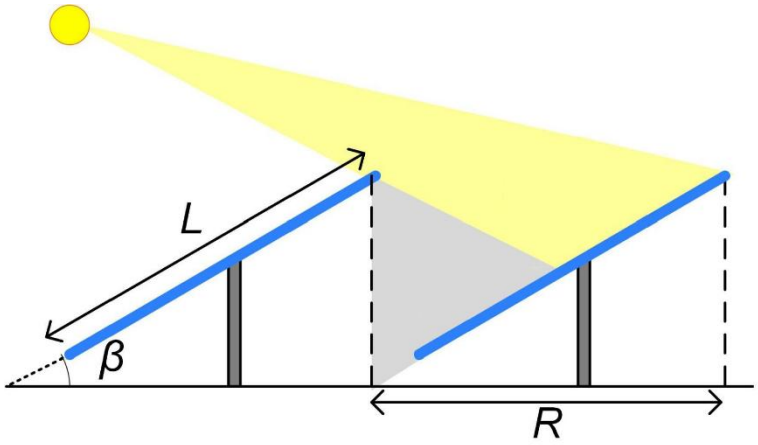

Figure 6. Ground cover ratio [69]

Increasing row-to-row pitch (R) reduces the shading effect caused by arrays themself. So, energy production per panel area (kWh/m^2) increases for low GCRs. Higher GCR cause more inter-row

shading, which decreases panel efficiency. However, since the higher GCRs allow for more PV panels to be installed, they may produce more energy for the same roof area compared to lower GCRs. Design details, such as the required number of PV panels, inverters and the connection configuration of array strings, are given in Table 8 for various GCRs considered for this study. A schematic representation of PV array installation is depicted in Figure 7.

Table 8. PV panel design scenarios

GCR	Number of PV panels	Installed Capacity (kWp)	PV area (m^2)	Inverter	Array Configuration
0.60	2718	815.4	4457	6x125kW	151 Strings x 18 in series
0.55	2500	750	4099	5x125kW	125 Strings x 20 in series
0.50	2242	672.6	3676	5x125kW	118 Strings x 19 in series
0.45	2040	612	3345	4x125kW	102 Strings x 20 in series
0.40	1824	547.2	2991	4x125kW	96 Strings x 19 in series
0.35	1580	474	2591	3x125kW	79 Strings x 20 in series
0.30	1360	408	2230	3x125kW	68 Strings x 20 in series

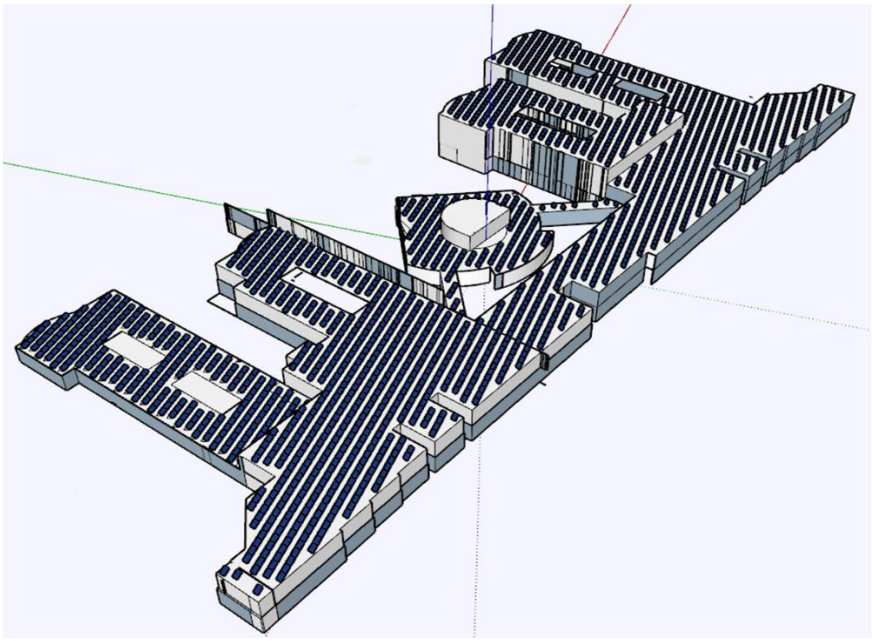

Figure 7. PV array installation layout

2.8. Performance indicators

In order to have better understanding of impact of onsite generation to electricity grid, a metric called grid interaction index (σ_{grid}) is widely used by researchers [70]. Grid interaction is

determined by considering two parameters: the net energy transfer to the grid and the average energy demand during that period. Net energy transfer is the difference between energy exported (E_{ex}) to grid and energy imported from grid (E_{im}). The average energy demand is the ratio of total energy consumption to the specified time period, usually monthly. Standard deviation of the ratio of these parameters referred to as grid interaction index (σ_{grid}). Low standard deviation is desired. Grid interaction and grid interaction index (σ_{grid}) can be calculated using Equations 4 and 5.

$$f_{grid,T} = \frac{E_{ex,i} - E_{im,i}}{\int_{t1}^{t2} E_i \, dt/T} \tag{4}$$

$$\sigma_{grid} = STD\ (f_{grid,T}) \tag{5}$$

Performance ratio (PR)is commonly calculated to evaluate the overall efficiency of a PV plant. It is basically the ratio between the actual and theoretical energy outputs of the PV plant. Since it accounts for all energy losses such as thermal losses, conduction losses or DC-AC conversion loss, it informs designers as to how energy efficient the PV plant is. Actual energy output of PV array is calculated as the sum of energy sent to grid ($E_{solar\ to\ grid}$) and energy sent to building ($E_{solar\ to\ building}$). The theoretical energy output is calculated by multiplying the average incident global irradiation (E_{global}) on PV plant by the nominal capacity of PV (PV_{nom}) which is determined at standard test conditions (1000 W/m², 25°C) [71].

$$PR = \frac{E_{solar\ to\ grid} + E_{solar\ to\ building}}{E_{global} * PV_{nom}} \tag{6}$$

Another indicator that shows how much of the load is covered by PV production is solar factor (ϕ_s). This fraction gives an idea about matching characteristics of generation (E_{gen}) and load (E_{load}) profiles. It indirectly shows how much of the demand must be covered by additional sources, such as grid for this study, since no energy storage is employed. The solar factor can be defined for an arbitrary time interval as;

$$\varphi_s = \frac{\sum_{t1}^{t2}(E_{gen}(t) - E_{net}(t))}{\sum_{t1}^{t2} E_{load}(t)} \tag{7}$$

where;

$$E_{net}(t) = \max\ [0, E_{gen}(t) - E_{load}(t)] \quad (8)$$

Energy use intensity (EUI) is a key performance indicator that represents the total amount of energy (E_{load}) consumed by the building per gross floor area (GFA) [72]. This value can serve as a benchmark for assessing the building's energy performance and for comparing it with relevant energy performance standards. It is calculated as follows:

$$EUI = \frac{E_{load}}{GFA} \quad (9)$$

2.9. Economic analysis

Life Cycle Cost Analysis (LCCA) is a widely used economical evaluation method [73]. It is a detailed analysis that considers present value of all cash flows over the lifespan of project. Initial investment costs, maintenance costs, replacement costs of equipment, energy costs or revenue and residual value of equipment are the main parameters considered in LCCA. Life cycle cost (LCC) of a project can be calculated according to Equation 10 [74].

$$LCC = IC + PV_{o\&m} + PV_{repl} + +PV_{energy} - PV_{res} \quad (10)$$

In Equation 10, IC represents the total investment costs for all equipment used in the project. For this study, IC encompasses the costs of PV panels and inverters, structural components for mounting the PV array on the roof, and electrical components, including conductors, conduit and fittings, transition boxes, switchgear, and panel boards. $PV_{o\&m}$ refers to maintenance costs, which include operation, repair and servicing costs of the equipment. It is assumed that 1% of the initial investment cost corresponds to maintenance costs [75].

PV_{repl} represents the cost of replacing equipment at the end of its useful life. For this study, the building's service life is considered to be 50 years. Therefore, any equipment with a shorter lifespan than the building's must be replaced. Specifically, with the service lives of PV panels and inverters being 25 years and 10 years, respectively, PV panels will need to be replaced once, while inverters will require replacement four times during the building's lifespan.

PV_{energy} refers to the cost associated with energy consumption for the building. In this study, energy consumption and generation occur simultaneously. Solar panels provide a portion of the energy needs, while the remaining portion is supplied by the grid. If the energy generated exceeds the building's requirements, the surplus is sent to the grid. Consequently, at the end of each month, there are both an energy bill and energy income. The difference between these two figures is calculated as PV_{energy}. When energy income exceeds the energy bill, it reduces the Life Cycle Cost (LCC). The calculations account for the reduction in energy output due to the degradation of PV panels over the building's lifespan. PV_{res} represents the residual value of equipment at the end of its life and is assumed to be zero, as there is no available information on the disposal cost of PV systems in Türkiye [76].

Present value of all future cash flows calculated by Equation 11.

$$PV = A_0\, x \sum_{t=1}^{N} \left(\frac{1}{1+d}\right)^t \tag{11}$$

where, N is the service life of building. A_0 represents the costs at the base year. d denotes discount rate which is taken as 14.5% for this study.

Another economic metric is the simple payback period (SPP). This method provides a quick and straightforward assessment of the economic benefits of a project. It estimates the number of years required for cash flows to recover the initial investment costs [77]. The SPP, which is the ratio of the initial investment costs (IC) to the annual energy savings, can be calculated using Equation 12. Energy tariff (C_{tariff}) and other parameters used in the economic analysis are detailed in Table 9.

$$SPP = \frac{IC}{(E_{ex,yearly} - E_{im,yearly}) x\, C_{tariff}} \tag{12}$$

Table 9. Parameters used in economic analysis

Parameter	**Value**	**Unit**
PV Panel Cost	0.41	$/W

Inverter Cost	0.07	$/W
Structural components (racking)	0.11	$/W
Electrical components	0.13	$/W
OM&R Cost	1	%
Lifespan of Building	50	years
Lifespan of PV panel	25	years
Lifespan of Inverter	10	years
Discount Rate	14.5	%
Electricity tariff	0.127	$/kWh

2.10. Environmental impact analysis

In this study, analysis of carbon emissions due to PV array installation is carried out for each PV system. Life Cycle Assessment (LCA) is used to evaluate these emissions, offering a solid and comprehensive approach that considers all stages of a product or service throughout its entire [78]. The key phases of this assessment are illustrated in Figure 8.

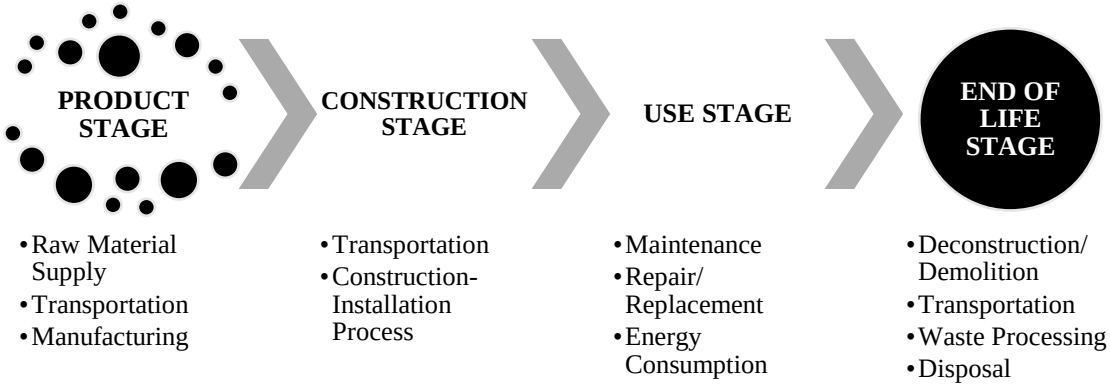

Figure 8. System boundary of life cycle assessment [79]

The product stage encompasses resource extraction, raw material production, and panel manufacturing. Carbon emissions during this stage are significantly influenced by the technology used and the energy mix of the grid. Different PV panel manufacturing technologies require varying amounts of energy, which affects the associated carbon emissions [80]. Additionally, the carbon intensity of the electricity grid plays a role; grids primarily powered by fossil fuels tend to have higher carbon emissions compared to those with a greater share of renewable energy sources. For this study, considering the type of PV panels used and Türkiye's grid mix, the carbon

emissions for the product stage are estimated at 125 kg.CO_2e/m^2 [81]. The carbon emission factor for electricity generation in Türkiye is taken as 0.689 kg.CO_2e/kWh [82].

Carbon emissions associated with transporting materials from a PV manufacturing factory to university campus were taken into account as well. Tractor-trailers used for regional deliveries, with a gross vehicle weight exceeding 16 tons, emit 863 grams of CO_2 per kilometer [83]. The distance between the manufacturing facility in Antalya, Türkiye, and the university campus is 700 kilometers.

Based on the information provided from the study by NREL on the life cycle greenhouse gas emissions from solar photovoltaics (PV), 60%-70% of total carbon emissions occur from the raw material extraction phase through to the operational stage of PV systems [84]. Operation and maintenance period account for 21%-26% of total emissions whereas end of life operations such as dismantling or disposal account for 5%-20% of total emissions. For this study, it is assumed that 25% of the total emissions occur during the use phase and 5% during the end-of-life phase.

An important metric for carbon emission is the carbon payback time (CPBT) [85]. It is essentially the time required for a PV system to counterbalance the amount of carbon emitted over its life cycle [86]. Carbon neutrality is achieved when the cumulative reduction in carbon emissions from the electricity generated by the PV system surpasses the system's total life cycle carbon emissions. The CPBT is influenced by both the carbon intensity of the grid and the level of solar irradiance.

3. RESULTS AND DISCUSSION

3.1 Building Energy Analysis

The comprehensive energy analysis reveals that the building's total annual energy consumption (E_{load}) is 626,656.47 kWh. The calculated EUI, based on site energy use, is 16.39 kWh/m² per year. This corresponds to a primary energy consumption of 29.41 kWh/m² per year, using a conversion factor of 1.794 [82].This primary energy metric is also known as the source EUI value. The concept of Nearly Zero-Energy Buildings (nZEBs) defines buildings with minimal energy usage throughout the year [87]. European countries have established specific nZEB standards according to their climate conditions, with source EUI values for non-residential buildings ranging from 21 kWh/m² to 176 kWh/m² [88]. The faculty building's EUI of 29.41 kWh/m² falls well within the

nZEB range established by the European Union, making it more feasible to offset energy consumption with renewable energy sources.

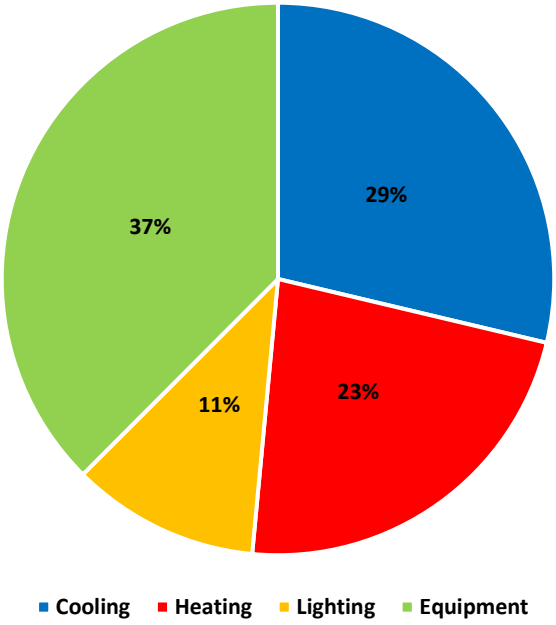

Figure 9. Energy consumption distribution

Share of energy consumption is given in Figure 9. The annual heating consumption for the engineering faculty building was calculated as 142,729.44 kWh whereas the annual cooling consumption was obtained to be 179,935.85 kWh for the hot seasons. The non-operational status of classrooms for educational purposes affects the cooling demand in summer season. Classrooms that are often not used in the summer cause the cooling load to be lower than expected. In other words, if there was an occupancy schedule similar to the education season in the summer season, it was evaluated that the cooling load could increase and be the dominant load. Osmaniye province experiences warm winters and hot and humid summers, which contributes to the cooling consumption. Combined, these factors result in a higher annual cooling load compared to the heating consumption in studied building.

The lighting energy consumption, which includes the energy consumption of artificial lighting systems, was found to be 68,901.43 kWh annually. This relatively low value is due to the building's minimal use after sunset and the presence of skylights in the corridors, which reduce the need for artificial lighting. he energy consumption of electrical equipment, which includes

devices such as computers, printers, and projectors, constitutes the largest portion of the building's energy use, totaling 235,089.75 kWh. It is crucial to review the energy consumption analysis monthly, as the consumption varies from month to month. Figure 10 shows the monthly variation in energy consumption, highlighting a decrease in both electrical equipment and lighting energy use during the summer months, attributed to lower occupancy rates and reduced usage in certain areas.

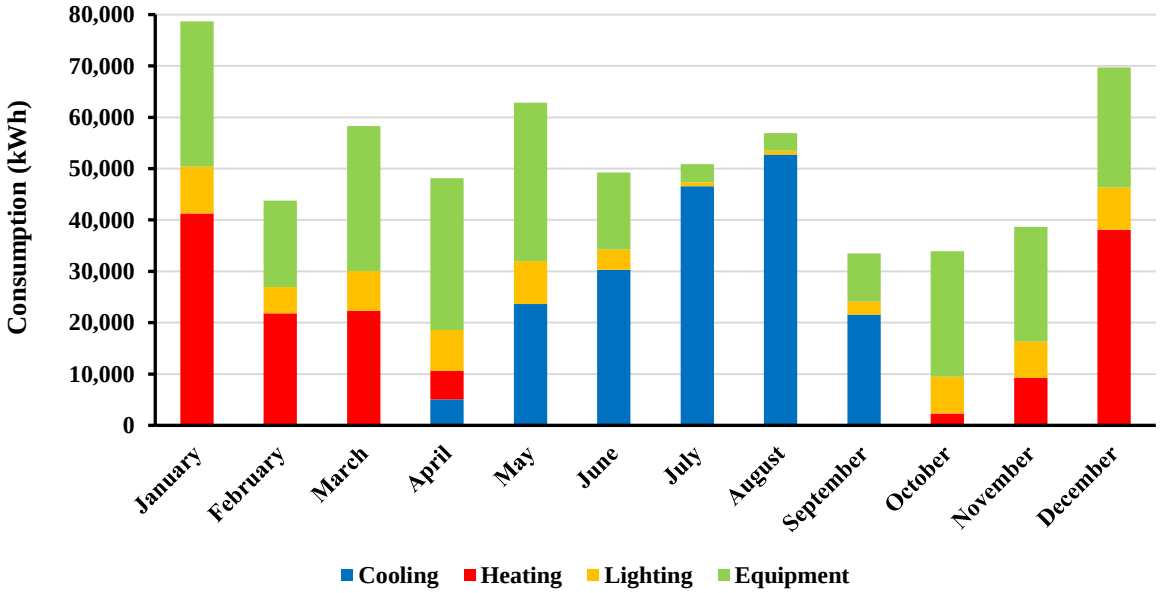

Figure 10. Monthly energy consumptions

Monthly fluctuations in energy consumption are influenced by variations in the building's usage schedule and weather conditions. For instance, in February, the heating energy consumption of the building decreases, primarily due to the closure of the classroom zones from January 22 to February 15. This specific usage condition leads to a reduction in the overall energy consumption and alters the energy characteristics of the building during that period.

3.2 Energy generation analysis

Monthly energy generation profiles for each GCR is presented in Figure 11. As expected, energy generation aligns with the seasonal variations in solar irradiance depicted in Figure 5. Additionally,

the monthly energy generation is proportional to the GCRs; as the GCR increases, so does the amount of energy generated each month.

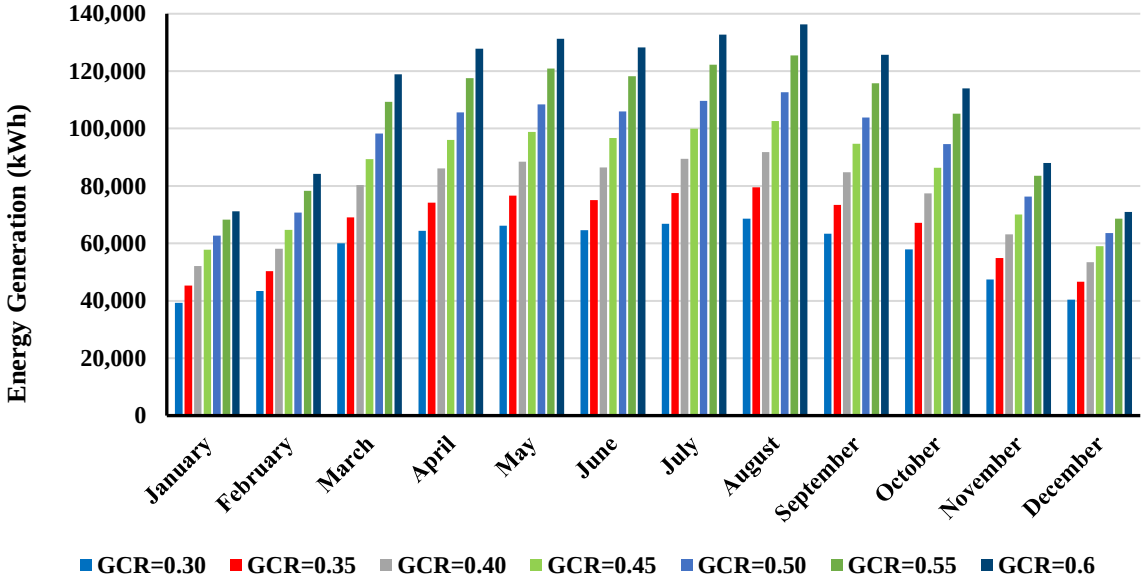

Figure 11. Monthly energy generation profiles

The analyzed PV model is able to supply energy to both the building and the grid. The building's energy needs (E_{load}) are met by two primary sources; the solar system installed on the roof and the grid. Energy is simultaneously drawn from these two sources. When the energy supplied by the solar system ($E_{solar\ to\ building}$) is insufficient to meet the building's demand, the grid compensates by providing additional energy ($E_{grid\ to\ building}$). If the energy generated by the PV system (E_{gen}) exceeds the building's demand, the surplus energy ($E_{solar\ to\ grid}$) is sent to the grid, as no energy storage system is modeled in this study. The difference between energy demand (E_{load}) and energy generation (E_{gen}) is referred to as the energy balance (E_{net}). Table 10 contains all energy interaction data for various GCRs.

Table 10. Yearly energy analysis

GCR	E_{gen} (kWh)	$E_{solar\ to\ building}$ (kWh)	$E_{solar\ to\ grid}$ (kWh)	$E_{grid\ to\ building}$ (kWh)	E_{net} (kWh)
0.60	1,329,297	514,908	814,389	111,749	702,640
0.55	1,233,414	509,308	724,107	117,349	606,758
0.50	1,112,401	498,298	614,103	128,359	485,744

0.45	1,016,088	486,541	529,546	140,116	389,430
0.40	911,658	469,239	442,419	157,418	285,001
0.35	789,600	442,079	347,521	184,578	162,943
0.30	682,318	408,849	273,469	217,808	55,661

Despite the presence of a solar energy system, the faculty building also imports electricity from the grid. Limited solar production during winter due to reduced daylight and cloud cover, along with late sunrises and peak demand periods, necessitate grid supplementation. However, the building achieves a net positive energy balance annually for all studied GCRs as indicated in Table 10. Increasing the GCR decreases the building's reliance on the grid. However, even at higher GCR values, the solar system does not fully meet the building's energy needs (E_{load}). For GCR values above 0.40, more than half of the generated energy (E_{gen}) is sent to the grid. At GCR values of 0.55 and 0.60, the total energy exported to the grid ($E_{solar\ to\ grid}$) exceeds the building's annual energy consumption (E_{load}).

Solar factors for each GCR are calculated using Equation 7 and presented in Table 11. This equation combines the factors of $E_{load,}$ E_{gen}, and E_{net} to yield a numerical value that reflects the effectiveness of solar energy utilization. While solar energy meets a significant portion of the building's energy needs, it does not fully cover all energy consumption.

Table 11. Solar factors

GCR	φ_s
0.60	82.17%
0.55	81.27%
0.50	79.52%
0.45	77.64%
0.40	74.88%
0.35	70.55%
0.30	65.24%

In addition to the cumulative annual solar factors for each GCR scenario presented in Table 11, specific days within the year were selected to closely examine the hourly relationship between load and generation profiles. January 14th and June 1st were chosen because they represent both low and high solar factor levels, respectively, and both days feature full building occupancy, unlike periods during semester breaks or summer holidays. Hourly load and generation profiles, along with hourly solar factors, are illustrated in Figures 12 and 13.

a)

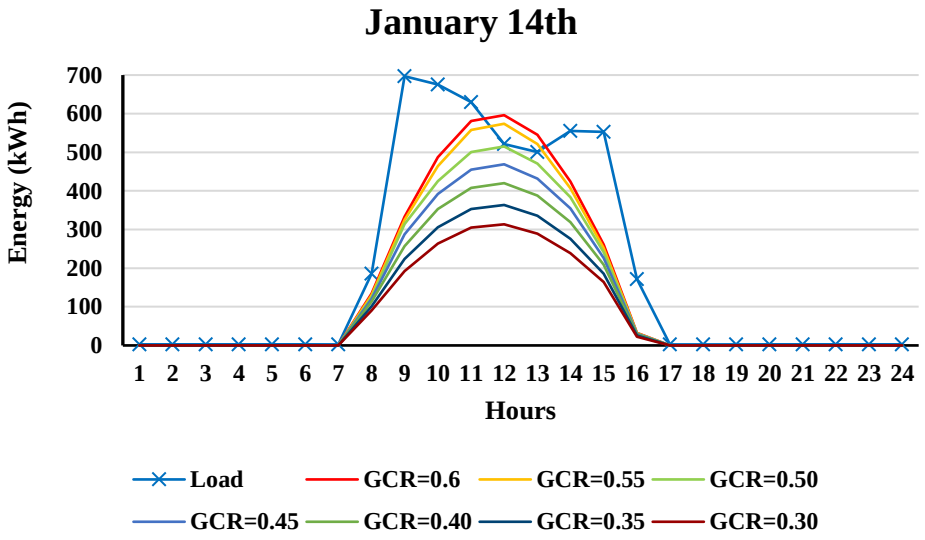

b)

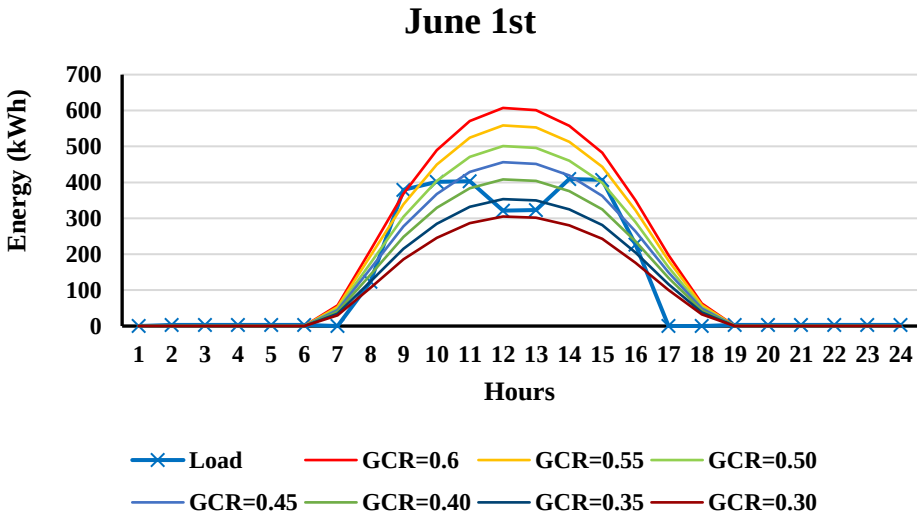

Figure 12. Energy profiles a) for January 14th and b) for June 1st

Figure 12 displays the solar energy generation for January 14th, revealing that the energy produced is insufficient to meet the building's consumption for most of the day. However, around noon, PV arrays with GCRs of 0.60 and 0.50 were able to provide adequate energy to the building for a period. In contrast, on June 1st, most scenarios with varying GCRs resulted in surplus energy generation, unlike January 14th according to Figure 12.

a)

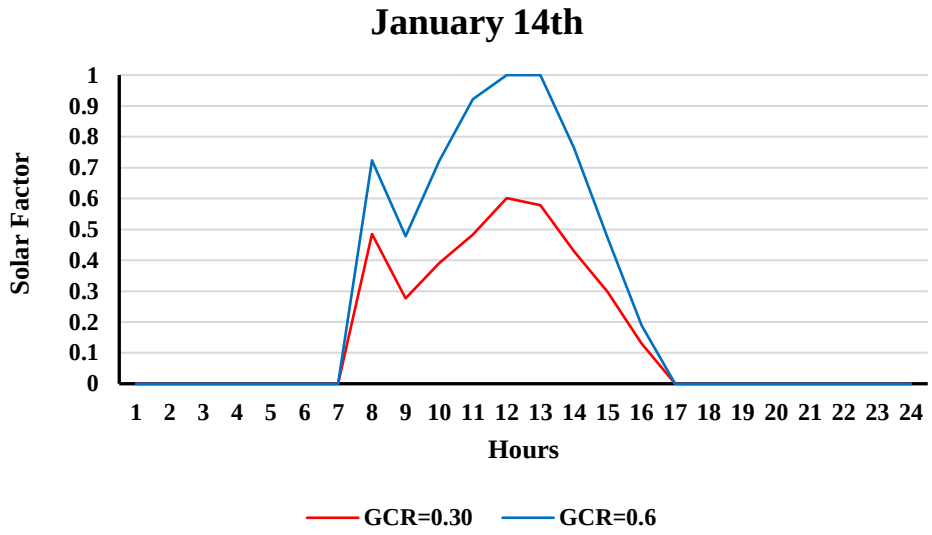

b)

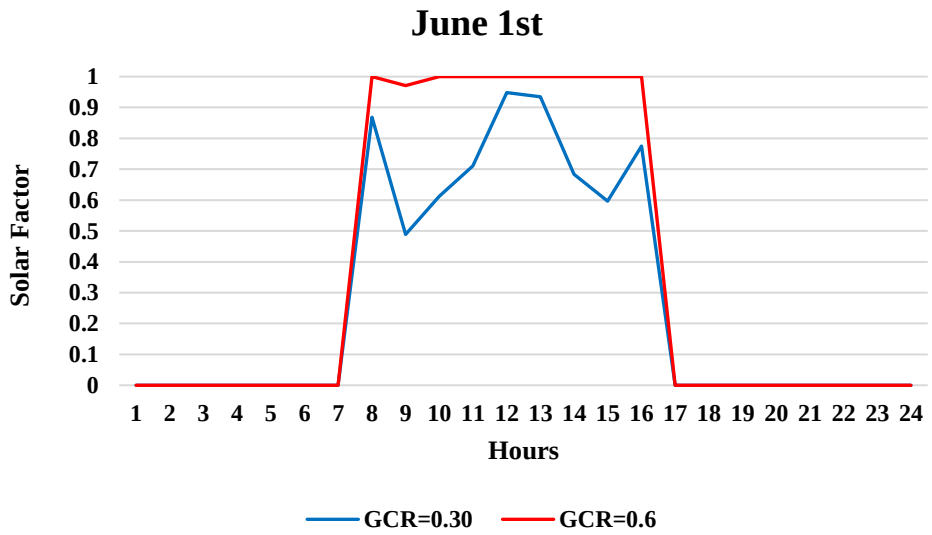

Figure 13. Solar factor a) for January 14th and b) for June 1st

For ease of graphical representation, Figure 13 illustrates the variation in solar factor for the highest and lowest GCRs. On June 1st, the average solar factor is 74% for a GCR of 0.30 and 99% for a GCR of 0.60. In contrast, on days with low solar irradiation levels, such as January 14th, the installed PV system capacity frequently falls short of meeting the building's energy demand throughout most of the day. For January 14th, the average solar factors are 40% for a GCR of 0.30 and 69% for a GCR of 0.60.

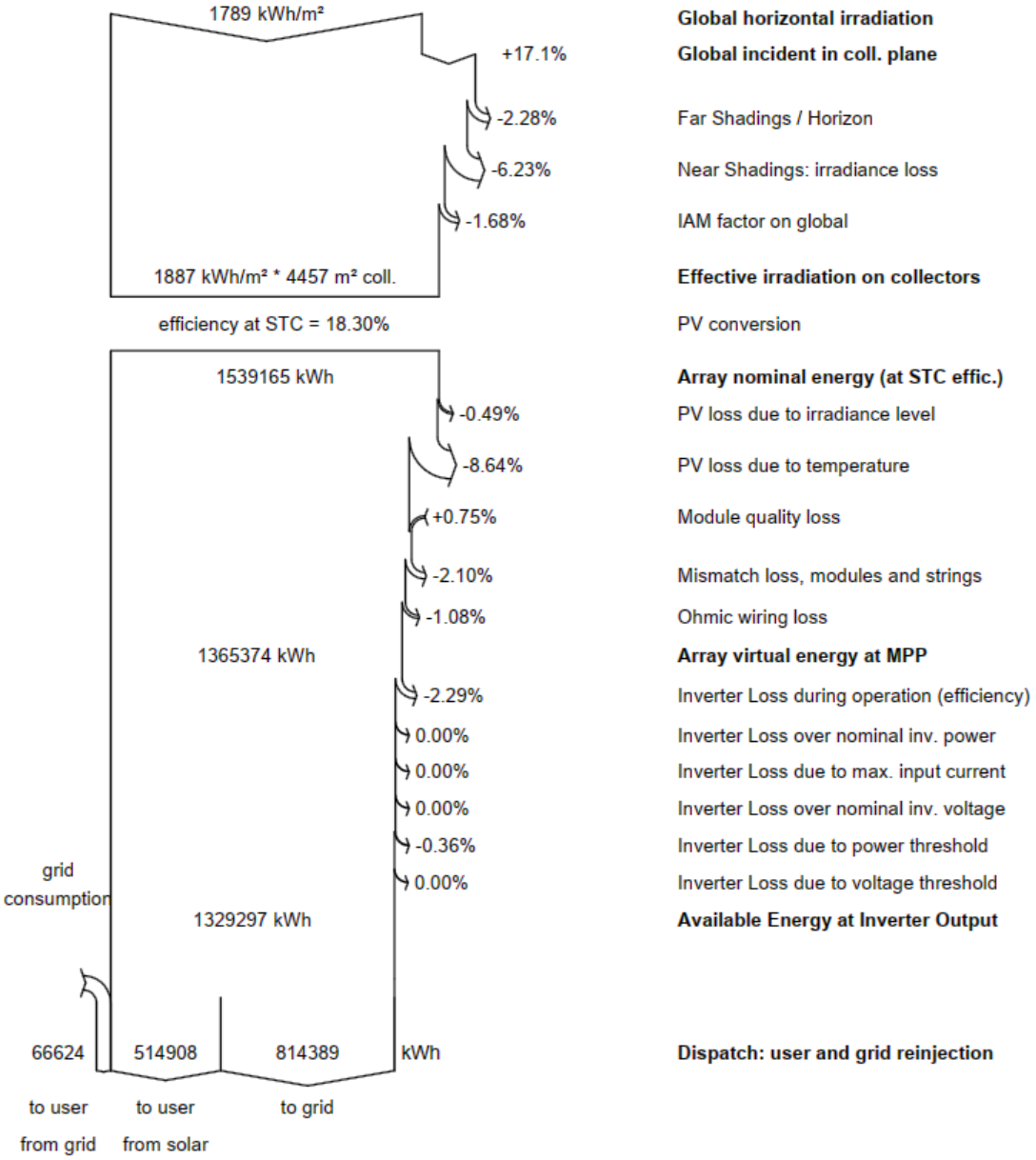

Figure 14. Loss diagram for GCR=0.60

Calculated main source of losses considered by PVsyst analysis tool for GCR=0.60 is illustrated in Figure 14. Figure 14 visualizes the breakdown of these losses, showing how array losses and inverter losses contribute to the overall efficiency of the PV system. It also depicts other factors such as wiring losses, temperature losses, and other miscellaneous losses. Array losses account for approximately 12.31%, whereas conversion losses are close to 3%.

Table 12 presents yearly average performance ratio values (PR), which is a critical metric to evaluate overall performance of PV system, along with specific production rate values (SP) which

is measured in terms of total energy generated per kilowatt-peak of installed capacity (kWh/kWp). PR values reported in Table 11 for the PV system, ranging from 77% to 79%, align closely with the range suggested by Lagarde et all [89]. As the system capacity increases, the performance ratio (PR) decreases due to higher array and conversion losses. Similarly, as the rows of the array become closer together, shading effects between rows increase, leading to a reduction in the SP.

Table 12. Performance ratios and specific production

GCR	PR	SP (kWh/kWp)
0.60	77.83%	1630
0.55	78.51%	1645
0.50	78.96%	1654
0.45	79.26%	1660
0.40	79.44%	1666
0.35	79.53%	1666
0.30	79.84%	1672

Cubukcu and Gumus reported a specific production of 1652.06 kWh/kWp for a grid-connected PV system located in the eastern part of Türkiye, based on a one-year real data analysis [90]. Comparable results were achieved through realistic simulations in this study, as presented in Table 12.

Eke and Demircan observed the year-round performance of a grid-connected PV system, achieving a performance ratio of 72% under the climate conditions of Muğla, Türkiye [91]. Sevik reported a performance ratio of 78.7% for the Çorum region, Türkiye [33], while Aktas and Ozenc calculated it as 84% for Siirt, Türkiye [31]. Therefore, the performance ratios for this study, as shown in Table 12, fall within the range observed in other studies for the climate conditions of Türkiye.

To evaluate the impact of the PV system on the grid, grid interaction indexes (σ_{grid}) for each GCR are calculated using Equation 4 and Equation 5. Although there is no universally defined recommended range for σ_{grid}, lower values are generally preferred as they indicate better grid integration and performance. Figure 15 shows that σ_{grid} starts at a low value of 0.14 with a GCR of 0.30. As the GCR increases, indicating more shading or obstruction, σ_{grid} rises proportionally,

reaching up to 0.43. This trend suggests that increased inter-row shading reduces PV system efficiency and presents greater challenges for maintaining stable grid interaction.

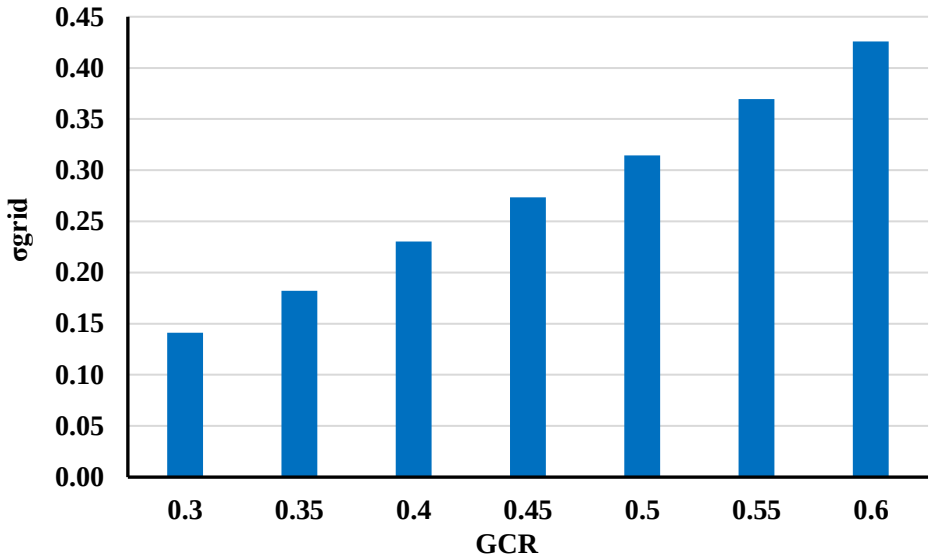

Figure 15. Grid interaction indexes

3.3 Life cycle cost analysis

A Life Cycle Cost Analysis (LCCA) was conducted to assess the total costs associated with investing in a solar energy system over the building's entire lifespan (50 years). This analysis includes various expenses incurred throughout the system's life. Figure 16 illustrates the breakdown of these expenses in LCC. According to Figure 16, the initial investment cost represents the largest portion of the total cost, followed by replacement costs for PV panels or inverters at the end of their useful life. Operation, maintenance, and repair (OM&R) costs, which cover monitoring, cleaning, and upkeep, account for the smallest share. Since some energy is supplied to the building from the grid, the associated energy bills also contribute to the LCC. Initial costs, OM&R, and replacement costs are directly proportional to the GCR, as increasing the system size leads to higher expenses. However, as the GCR rises, meaning a larger portion of the energy needs is met by on-site generation, the energy costs decrease. Consequently, reduced grid purchases result in direct savings on energy costs.

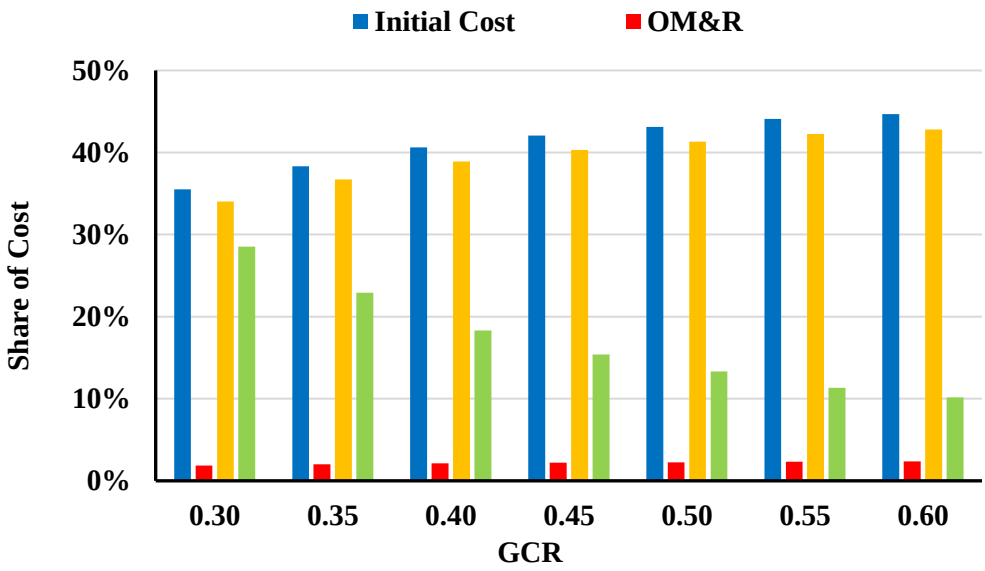

Figure 16. Share of expenses of LCC

The initial investment cost encompasses the purchase and installation of PV panels, inverters, solar mounting systems, and additional equipment such as cables and circuit breakers. Given its significant impact on the LCC, Figure 17 offers a detailed breakdown of how these components contribute to the overall initial investment. The cost of PV panels represents the largest portion of this investment, followed by expenses for structural components, electrical components, and inverters.

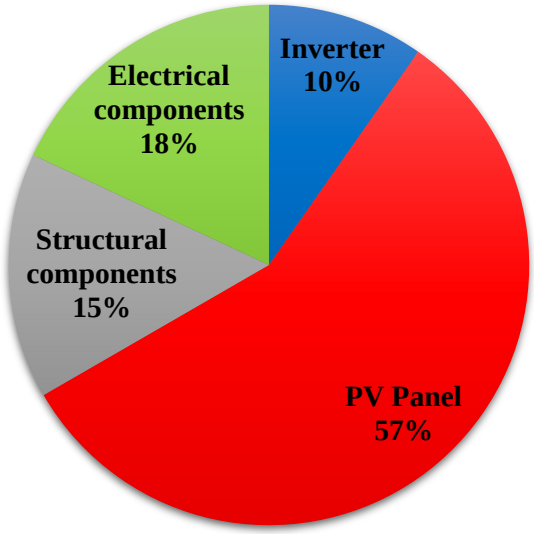

Figure 17. Distribution of initial investment cost components

Since the system in this study can sell surplus electricity, it helps offset a portion of the LCC. Figure 18 presents a comparative analysis of LCC per unit of installed capacity (LCC/kWp) for different GCRs, along with the total revenue generated from selling energy back to the grid. Higher GCRs optimize the use of available roof space for PV panels, maximizing total energy production per unit area. This increased energy yield relative to the total system cost results in a lower LCC/kWp. Additionally, greater electricity generation creates extra revenue streams, improving the economic feasibility of the PV installation. Therefore, higher GCRs offer significant economic benefits by reducing LCC/kWp and increasing revenue from grid sales.

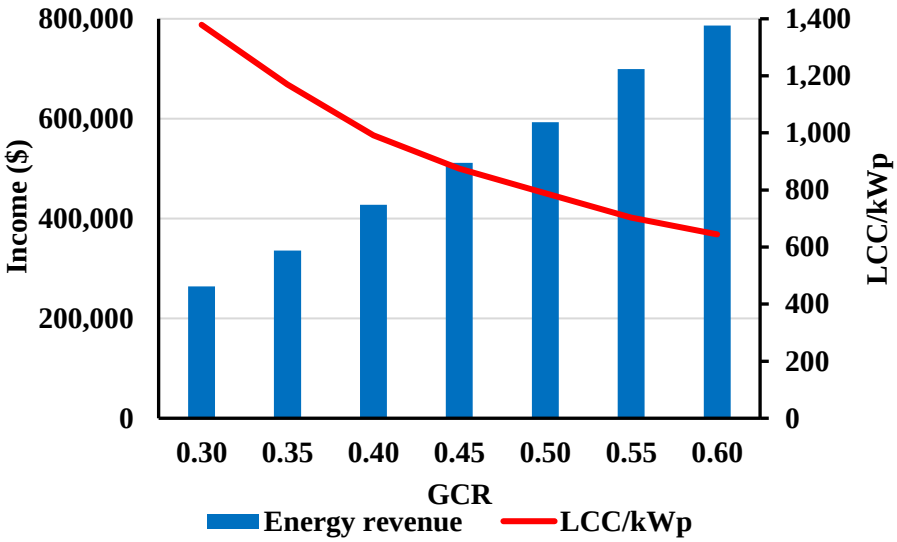

Figure 18. Energy generation revenue and LCC/kWp

Higher GCRs not only enhance energy production and revenue but also lead to shorter payback periods for the initial investment. According to Figure 19, simple payback time decreases to 6.5 years for GCR=0.6. Shorter payback periods make these solutions more financially viable and support the achievement of both economic and environmental sustainability goals.

Duman and Güler found that a 5kW rooftop PV system for residential buildings in southern Türkiye has a payback period of 7.75–8.33 years based on 2020 economic data.[92]. Alıç calculated the payback period for a PV system of the same size in Kahramanmaraş as 8.38 years. [34].

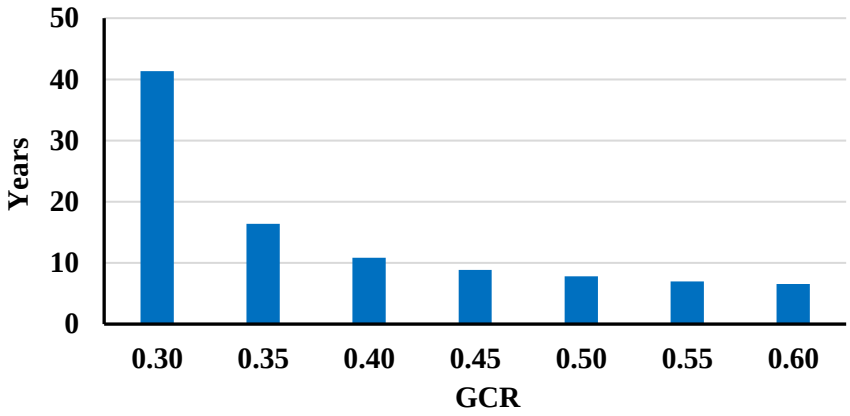

Figure 19. Payback period

3.4 Life cycle CO_2 analysis

The CO_2 emissions for the base case, where no renewable energy is installed, represent the scenario where the building's energy demand is fully met by the grid, resulting in no avoided or reduced CO_2 emissions. The total CO_2 emissions for this base case are calculated using the carbon emission factor. Despite installing various PV panels on the roof to reduce grid dependency, some energy is still drawn from the grid, meaning that CO_2 emissions continue as the grid cannot provide entirely carbon-free energy. Another key parameter is avoided CO_2 emissions, which represents the amount of CO_2 emissions that have been prevented due to the integration of the renewable energy system. The energy generated by the PV system is directly factored into the calculation of avoided CO_2 emissions. The difference between the CO_2 emissions from the grid and the avoided CO_2 emissions is referred to as Net CO_2 emissions, reflecting the overall impact on CO_2 emissions. Figure 20 presents all these parameters along with the base case data.

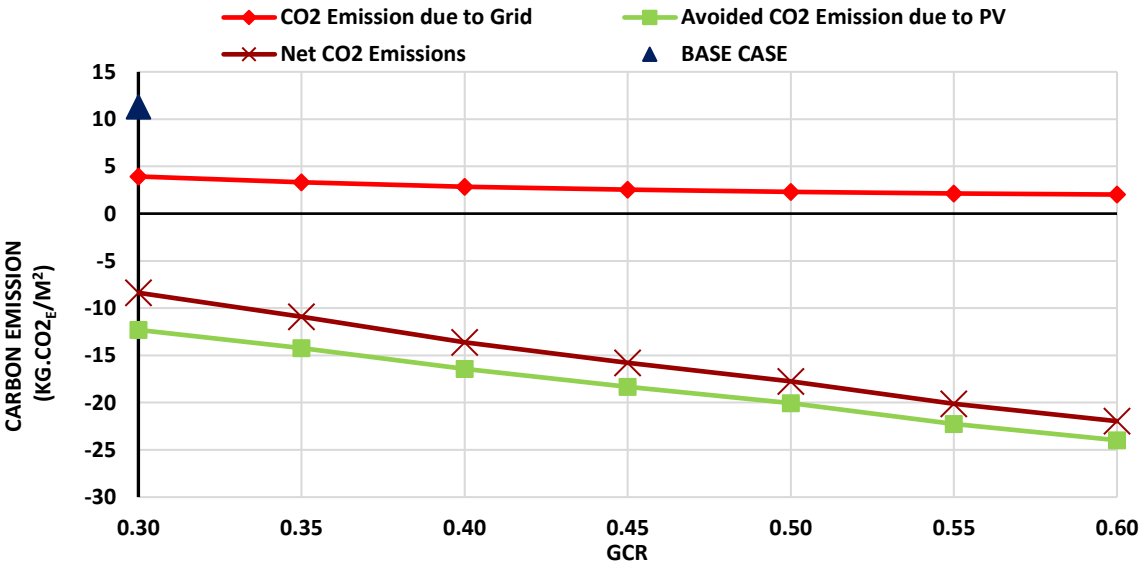

Figure 20. Energy generation revenue and LCC/kWp

As the GCR increases, the energy supplied to the building by the PV system also rises, leading to reduced energy drawn from the grid. This decrease in grid electricity consumption results in lower CO_2 emissions associated with grid-supplied energy. Concurrently, avoided CO_2 emissions from the PV system increase as higher GCRs enable more electricity generation. This is because the PV system replaces grid electricity that would otherwise be generated from fossil fuels. When avoided CO_2 emissions surpass the CO_2 emissions from grid electricity, net CO_2 emissions become negative, as illustrated in Figure 20, indicating a net reduction in CO_2 emissions due to the renewable energy integration. As the GCR continues to increase, both CO_2 emissions from grid electricity and net CO_2 emissions decrease, reflecting a reduction in the building's dependence on fossil fuel-based grid electricity and resulting in lower overall CO_2 emissions.

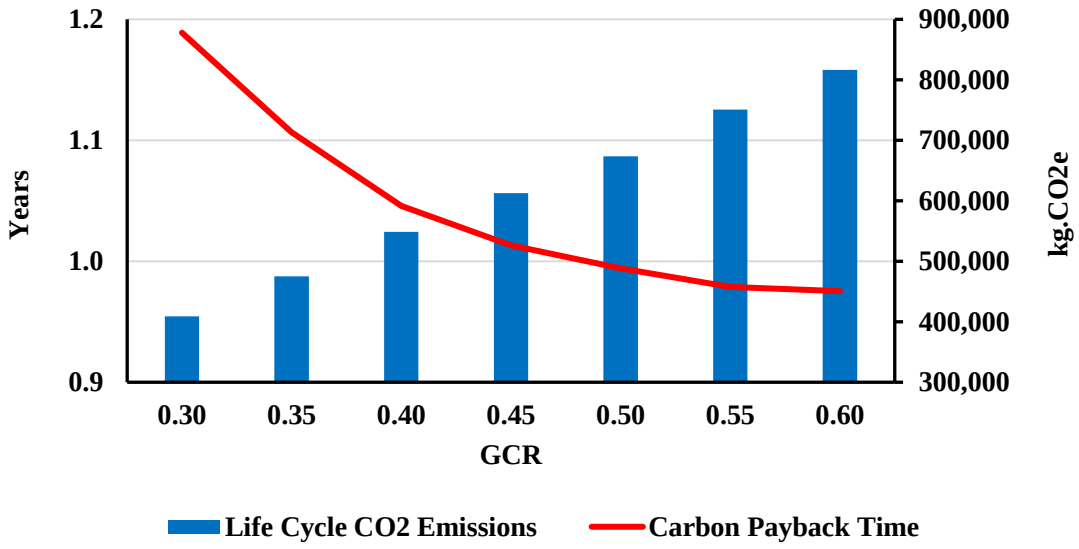

Figure 21. Carbon payback period

Figure 21 plots the carbon payback times, which represent the duration needed for the cumulative CO_2 emissions avoided to match or exceed the total CO_2 emissions produced over the building's entire life cycle. Studies have demonstrated that the average carbon payback period for solar panels ranges from 1 to 4 years [93].The data in Figure 21 indicates that the building generally achieves carbon neutrality in CO_2 emissions by the end of its first operational year. However, with a higher ground cover ratio, it takes longer to offset carbon emissions due to reduced specific electricity

generation from PV panels and higher life cycle CO_2 emissions. The rate at which carbon neutrality is achieved varies with the GCR.

4. CONCLUSION

This study evaluates the integration of rooftop photovoltaic (PV) systems into a faculty building in Osmaniye, Türkiye, which meets Nearly Zero-Energy Building (nZEB) standards with a source energy use intensity (EUI) of 29.41 kWh/m²/year. The analysis reveals that the building's energy demand is dominated by cooling due to its operational patterns and the region's hot climate, with summer reductions attributed to unoccupied classrooms. A detailed PV system simulation, accounting for varying ground cover ratios (GCRs), demonstrates net-positive annual energy generation across all scenarios. Systems with GCRs exceeding 0.40 export over 50% of their production to the grid, achieving a performance ratio of 77–79% and specific yields of 1630–1672 kWh/kWp. However, larger systems face efficiency declines from shading and conversion losses.

Economically, higher GCRs maximize revenue through grid exports, reducing the life cycle cost per kWp and yielding a payback period as short as **6.5 years** (GCR 0.6). Environmentally, the PV system offsets grid reliance, achieving carbon neutrality within one year of operation. While higher GCRs extend carbon payback periods slightly due to increased embodied emissions, they still enable significant net CO_2 reductions. These findings emphasize the importance of optimizing GCR to balance energy output, economic viability, and environmental impact.

This methodology, adaptable to diverse building types and climates, provides a scalable framework for advancing zero-energy buildings and supporting global carbon reduction strategies. By prioritizing system design tailored to local conditions, stakeholders can enhance renewable energy adoption in the built environment.

NOMENCLATURE

AC	alternating current
ASHRAE	American society of heating, refrigerating, and air-conditioning engineers
CDD	cooling degree days
COP	coefficient of performance
CPBT	carbon payback time

DC	direct current
EUI	energy use intensity
FiT	feed-in tariffs
GCR	ground cover ratio
GWP	global warming potential
HDD	heating degree days
HVAC	heating, ventilating, and air conditioning
IESNA	illuminating engineering society north America
LCA	life cycle assessment
LCCA	life cycle cost analysis
NREL	national renewable energy laboratory
PV	photovoltaic(s)
SPP	simple payback period
TMY	typical meteorological year
USD	U.S. dollars
VDC	volts direct current
VRF	variable refrigerant flow
WAC	watts alternating current
WDC	watts direct current
Wp	watts peak
WWR	window-to-wall ratio
ZEB	zero energy building

DECLARATION OF ETHICAL STANDARDS

The authors of the paper submitted declare that nothing which is necessary for achieving the paper requires ethical committee and/or legal-special permissions.

CONTRIBUTION OF THE AUTHORS

Muhammed Enes Umcu: Building energy model and PV model. Writing original draft.

Ugur ACAR: Checking models accuracy, making subsequent calculations, editing the whole manuscript.

Önder KAŞKA: Supervising the whole process.

CONFLICT OF INTEREST

There is no conflict of interest in this study.

REFERENCES

[1] Pérez-Lombard L, Ortiz C. Pout C. A review on buildings energy consumption information. Energy and Buildings 2008; 40(3): 394-398.

[2] Sayın S. The Significance of the use of renewable energy in our country's building sector and the opportunities of utilizing of solar energy in buildings. Selcuk University. M. Sc. Thesis, 2006.

[3] Eurostat. Accessed on the date of: 22.01.2023; Available from: https://ec.europa.eu/eurostat/cache/infographs/energy_balances/enbal.html.

[4] MENR, M.O.E.A.N.R. National Energy Efficiency Action Plan (2017–2023). Accessed on the date of; Available from: https://www.resmigazete.gov.tr/eskiler/2018/01/20180102M1-1-1.pdf.

[5] Yildiz Y,M Koçyiğit. Energy consumption analysis of education buildings: The case study of Balikesir University. Gazi University Journal of Science 2021;34:665-677.

[6] Alshuwaikhat HM, Abubakar I. An integrated approach to achieving campus sustainability: assessment of the current campus environmental management practices. Journal of Cleaner Production 2008; 16(16): 1777-1785.

[7] Barbhuiya S, Barbhuiya S. Thermal comfort and energy consumption in a UK educational building. Building and Environment 2013; 68: 1-11.

[8] Goenaga-Pérez A, Álvarez-Sanz M, Terés-Zubiaga J, Campos-Celador A. Cost-effectiveness and minimum requirements of nZEB for residential buildings under the new Spanish Technical Building Code. Energy and Buildings 2023; 287: 112986.

[9] Hassan J, Zin R , Abd Majid M, Balubaid S, Hainin M. Building energy consumption in Malaysia: An overview. Jurnal Teknologi 2014; 70(7).

[10] Kitsopoulou A, Pallantzas D, Sammoutos C, Lykas P, Bellos E, Vrachopoulos MG, Tzivanidis C. A comparative investigation of building rooftop retrofit actions using an energy and computer fluid dynamics approach. Energy and Buildings 2024; 315: 114326.

[11] Naserabad, SN, Ahmadi P, Mobini K, Mortazavi M. Thermal design and dynamic performance assessment of a hybrid energy system for an educational building. Energy and Buildings 2023; 278: 112513.

[12] Zafaranchi M, Sozer H. Enhancing energy efficiency through hourly assessments of passive interventions in educational-office buildings: A case study in a Mediterranean climate. Energy Reports 2024; 11: 423-441.

[13] Heracleous C, Michael A, Savvides A, Hayles C. A methodology to assess energy-demand savings and cost-effectiveness of adaptation measures in educational buildings in the warm Mediterranean region. Energy Reports 2022; 8: 5472-5486.

[14] Javid AS, Aramoun F, Bararzadeh M, Avami A. Multi objective planning for sustainable retrofit of educational buildings. Journal of Building Engineering 2019; 24: 100759.

[15] Ilham NI, Dahlan NY, Hussin MZ. Optimizing solar PV investments: A comprehensive decision-making index using CRITIC and TOPSIS. Renewable Energy Focus 2024; 49: 100551.

[16] Anoune K, Bouya M, Astito A, Abdellah AB. Sizing methods and optimization techniques for PV-wind based hybrid renewable energy system: A review. Renewable and Sustainable Energy Reviews 2018; 93: 652-673.

[17] Fiorotti R, Yahyaoui I, Rocha HR, Honorato Í, Silva J, Tadeo F. Demand planning of a nearly zero energy building in a PV/grid-connected system. Renewable Energy Focus 2023; 45: 220-233.

[18] Emil F, Diab A. Energy rationalization for an educational building in Egypt: Towards a zero energy building. Journal of Building Engineering 2021; 44: 103247.

[19] Koo C, Shi K, Li W, Lee J. Integrated approach to evaluating the impact of feed-in tariffs on the life cycle economic performance of photovoltaic systems in China: A case study of educational facilities. Energy 2022; 254: 124302.

[20] Taghavifar H, Zomorodian ZS. Techno-economic viability of on grid micro-hybrid PV/wind/Gen system for an educational building in Iran. Renewable and Sustainable Energy Reviews 2021; 143: 110877.

[21] Suarez-Ramon I, Alvarez-Rodriguez M, Ruiz-Manso C, Perez-Dominguez F, Gonzalez-Vega P. A general sizing methodology of grid-connected PV systems to meet the zero-energy goal in buildings. Energy 2024: 132580.

[22] Omar A, Khattab N, Abdel Aleem S. Optimal strategy for transition into net-zero energy in educational buildings: A case study in El-Shorouk City, Egypt. Sustainable Energy Technologies and Assessments 2021; 49: 101701.

[23] Khairi NHM, Akimoto Y, Okajima K. Suitability of rooftop solar photovoltaic at educational building towards energy sustainability in Malaysia. Sustainable Horizons 2022; 4: 100032.

[24] Park HS, Jeong K, Hong T, Ban C, Koo C, Kim J. The optimal photovoltaic system implementation strategy to achieve the national carbon emissions reduction target in 2030: Focused on educational facilities. Energy and Buildings 2016; 119: 101-110.

[25] Gbadamosi SL, Ogunje FS, Wara ST, Nwulu NI. Techno-economic evaluation of a hybrid energy system for an educational institution: a case study. Energies 2022; 15(15): 5606.

[26] Munguba C, Leite G, Ochoa A, Michima P, Silva H, Vilela O, Kraj A. Enhancing cost-efficiency in achieving near-zero energy performance through integrated photovoltaic retrofit solutions. Applied 1 Energy 2024; 367: 123307.

[27] Kabir MA, Hasan MM, Hossain T, Ahnaf A, Monir H. Sustainable energy transition in Bangladeshi academic buildings: A techno-economic analysis of photovoltaic-based net zero energy systems. Energy and Buildings 2024; 312: 114205.

[28] Michelle L, Chiara P. Assessing life cycle sustainability of building renovation and reconstruction: A comprehensive review of case studies and methods. Building and Environment 2024: 111817.

[29] Hemmati M, Bayati N, Ebel T. Integrated life cycle sustainability assessment with future energy mix: A review of methodologies for evaluating the sustainability of multiple power generation technologies development. Renewable Energy Focus 2024: 100581.

[30] Moazzen N, Karagüler ME, Ashrafian T. Comprehensive parameters for the definition of nearly zero energy and cost optimal levels considering the life cycle energy and thermal comfort of school buildings. Energy and Buildings 2021; 253: 111487.

[31] Aktas IS, Ozenc S. A case study of techno-economic and environmental analysis of college rooftop for grid-connected PV power generation: Net zero 2050 pathway. 1 Case Studies in Thermal Engineering 2024; 56: 104272.

[32] Özcan Ö, Duman AC, Gönül Ö, Güler Ö. Techno-economic analysis of grid-connected PV and second-life battery systems for net-zero energy houses. Journal of Building Engineering 2024; 89: 109324.

[33] Şevik S. Techno-economic evaluation of a grid-connected PV-trigeneration-hydrogen production hybrid system on a university campus. International Journal of Hydrogen Energy 2 2022; 47(57): 23935-23956. 3

[34] Alıç O. A holistic techno-economic feasibility analysis of residential renewable energy systems: An insight into Turkish case. Journal of Energy Storage 2024; 94: 112433.

[35] Bilir L,Yildirim N. Photovoltaic system assessment for a school building. International Journal of Hydrogen Energy 2017; 42(28): 17856-17868.

[36] Dal AÖ, Ashrafian T. Evaluation of Building Retrofitting Alternatives Towards Zero Energy School Building in Turkey. CLIMA 2022: the 14th REHVA HVAC World Congress, 1 Rotterdam, Netherlands, 2022.

[37] Atmaca A, Atmaca N. Life cycle energy (LCEA) and carbon dioxide emissions (LCCO2A) assessment of two residential buildings in Gaziantep, Turkey. Energy and Buildings 2 2015; 102: 417-431.

[38] Atmaca A, Atmaca N. Carbon footprint assessment of residential buildings, a review and a case study in Turkey. Journal of Cleaner Production 3 2022; 340: 130691.

[39] Kayaçetin, NC, Hozatlı B. Whole life carbon assessment of representative building typologies for nearly zero energy building definitions. Journal of Building Engineering 2024; 95: 110214.

[40] Kınay U, Laukkarinen A, Vinha J. Renovation wave of the residential building stock targets for the carbon-neutral: Evaluation by Finland and Türkiye case studies for energy demand. 4 Energy for Sustainable Development 2023; 75: 1-24.

[41] Kayaçetin NC, Tanyer AM. Embodied carbon assessment of residential housing at urban scale. Renewable and Sustainable Energy Reviews 2020; 117: 109470.

[42] Casini M. Chapter 5—Building performance simulation tools. Construction 2022; 4: 221-262.

[43] TS 825, Thermal insulation requirements for buildings. 2008, Turkish Standards Institution Ankara, Turkey.

[44] Almarzouq A, Sakhrieh A. Effects of glazing design and infiltration rate on energy consumption and thermal comfort in residential buildings. Thermal Science 2019; 23 (5 Part B): 2951-2960.

[45] Yu S, Cui Y, Xu X, Feng G. Impact of civil envelope on energy consumption based on EnergyPlus. Procedia Engineering 2015; 121: 1528-1534.

[46] Feng X, Yan D, Peng C, Jiang Y. Influence of residential building air tightness on energy consumption. HVAC 2014; 44: 5-14.

[47] Yao J, Huang Y, Cheng K. Coupling effect of building design variables on building energy performance. Case Studies in Thermal Engineering 2021; 27: 101323.

[48] Acar U, Kaska O, Tokgoz N.. Multi-objective optimization of building envelope components at the preliminary design stage for residential buildings 5 in Turkey. Journal of Building Engineering 2021; 42: 102499.

[49] Crawley D, Lawrie L. Development of Global Typical Meteorological Years (TMYx). Accessed on the date of: 01.04.2022; Available from: http://climate.onebuilding.org.

[50] Acar U, Kaşka Ö, Tokgöz N. The effects of different typical meteorological year data on the heating and cooling demand of buildings: case study of Turkey. 6 Journal of Thermal Engineering 2022; 8: 677-90.

[51] Öztürk MZ, Çetinkaya G, Aydın S. Köppen-Geiger iklim sınıflandırmasına göre Türkiye'nin iklim tipleri. Coğrafya Dergisi 2017(35): 17-27.

[52] TS825, Binalarda Isı Yalıtım Kuralları. 2008, Türk Standartları Enstitüsü.

[53] McClellan TM, Pedersen CO. Investigation of outside heat balance models for use in a heat balance cooling load calculation procedure. 7 Conference: American Society of Heating, Refrigerating and Air-Conditioning Engineers (ASHRAE) annual meeting, Boston, MA, United States, 1997.

[54] Rees SJ, Spitler JD, Davies MG, Haves P. Qualitative comparison of North American and UK cooling load calculation methods. HVAC&R Research 2000; 6(1): 75-99.

[55] ANSI, ASHRAE Standard 55 (2013) Thermal Environmental Conditions for Human Occupancy. 2013.

[56] Younes C, Shdid CA, Bitsuamlak G. Air infiltration through building envelopes: A review. Journal of Building Physics 2012; 35(3): 267-302.

[57] Speert J, Legge C. Informed Mechanical Design Through Tested Air Leakage Rates. in Building Enclosure Science & Technology (BEST3) Conference, 2012.

[58] Delzendeh E, Wu S, Lee A, Zhou Y. The impact of occupants' behaviours on building energy analysis: A research review. Renewable and Sustainable Energy Reviews 8 2017; 80: 1061-1071.

[59] Yazit RNSRM, Husini EM, Khamis MK, Zolkefli MF, Dodo YA. Illuminance level measurement at lower working plane height in Islamic religious school. Asian Journal of University Education 2020; 16(3): 125-137.

[60] Rea M. The IESNA Lighting handbook 9th ed. ed J. Block. New York: Publications Department IESNA, 2000.

[61] McKenney K, Guernsey M, Ponoum R, Rosenfeld J. Commercial miscellaneous electric loads: Energy consumption characterization and savings potential in 2008 by building 9 type. TIAX LLC, Lexington, MA, 10 Tech. Rep. D 2010; 498: 224.

[62] Wang L, Mathew P, Pang X. Uncertainties in energy consumption introduced by building operations and weather for a medium-size office building. Energy 11 and Buildings 2012; 53: 152-158.

[63] Energy, U., Buildings energy data book, in, 2012. 2011.

[64] Ghatikar G. Miscellaneous and electronic loads energy efficiency opportunities for commercial buildings: a collaborative study by the United States and 12 India. Report number: LBNL-6287E. Lawrence Berkeley National Laboratory and Infosys Technologies Limited, 2013.

[65] Frank S, Polese LG, Rader E, Sheppy M, Smith J. Extracting operating modes from building electrical load data. IEEE Green Technologies Conference (IEEE-Green). 2011.

[66] Bader S, Ma X, Oelmann B. One-diode photovoltaic model parameters at indoor illumination levels–A comparison. Solar Energy 2019; 180: 707-716.

[67] Acar U, Kaska O. Energy and economical optimal of Nzeb design under different climate conditions of Türkiye. Journal of Building Engineering 2022; 60: 105103.

[68] Feldman D, Ramasamy V, Fu R, Ramdas A, Desai J, Margolis R. US solar photovoltaic system and energy storage cost benchmark. National Renewable Energy Lab.(NREL), Golden, CO, United States, 2021.

[69] Doubleday K, Choi B, Maksimovic D, Deline C, Olalla C. Recovery of inter-row shading losses using differential power-processing submodule DC–DC converters. Solar Energy 2016; 135: 512-517.

[70] Huang Z, Lu Y, Wei M, Liu J. Performance analysis of optimal designed hybrid energy systems for grid-connected nearly/net zero energy buildings. 13 Energy 2017; 141: 1795-1809.

[71] Delgarm N, Sajadi B, Kowsary F, Delgarm S. Multi-objective optimization of the building energy performance: A simulation-based approach by means of particle swarm 14 optimization (PSO). Applied Energy 2016; 170: 293-3

[72] Andrews CJ, Krogmann U. Technology diffusion and energy intensity in US commercial buildings. Energy Policy 2009; 37(2): 541-553.

[73] Zhao J, Li S. Life cycle cost assessment and multi-criteria decision analysis of environment-friendly building insulation materials-A review. Energy and Buildings 1 2022; 254: 111582.

[74] Kneifel J, Lavappa P. Energy Price Indices and Discount Factors for Life-Cycle Cost Analysis–. Annual Supplement to NIST Handbook 2024; 135.

[75] CEN, EN 15459:2008 Standard- Energy performance of buildings - Economic evaluation procedure for energy systems in buildings. European Committee for Standardization, 2 2008.

[76] Or B, Bilgin G, Akcay EC, Dikmen I, Birgonul MT. Real options valuation of photovoltaic investments: A case from Turkey. Renewable and Sustainable Energy Reviews 2024; 192: 114200.

[77] Stevanović S, Pucar M. Investment appraisal of a small, grid-connected photovoltaic plant under the Serbian feed-in tariff framework. Renewable and Sustainable Energy Reviews 3 2012; 16(3): 1673-1682.

[78] Fenner AE, Kibert CJ ,Li J, Razkenari MA, Hakim H, Lu X, Kouhirostami M, Sam M. Embodied, operation, and commuting emissions: A case study comparing the carbon hotspots of an educational building. Journal of Cleaner Production 4 2020; 268: 122081.

[79] Fenner AE, Kibert CJ, Woo J, Morque S, Razkenari M, Hakim H, Lu X. The carbon footprint of buildings: A review of methodologies and applications. Renewable 5 and Sustainable Energy Reviews 2018; 6 94: 1142-1152.

[80] Raugei M, Bargigli S, Ulgiati S. Life cycle assessment and energy pay-back time of advanced photovoltaic modules: CdTe and CIS compared to poly-Si. Energy 7 2007; 32(8): 1310-1318.

[81] Wikoff HM, Reese SB, Reese MO. Embodied energy and carbon from the manufacture of cadmium telluride and silicon photovoltaics. Joule 2022; 6(7): 1710-1725.

[82] Accessed on the date of: 01.04.2024; Available from: https://meslekihizmetler.csb.gov.tr/elektrik-enerjisinin-birincil-enerji-ve-sera-gazi-salimi-katsayilari-i-100347.

[83] Ragon PL, Rodríguez F. CO2 emissions from trucks in the EU: An analysis of the heavy-duty CO2 standards baseline data, July 2019–June 2020. International Council on Clean Transportation, 2021.

[84] NREL, Life cycle greenhouse gas emissions from solar photovoltaics, National Renewable Energy Lab.(NREL), Golden, CO,United States, 2012.

[85] Wu F, Zhou Z, Temizel-Sekeryan S, Ghamkhar R, Hicks AL. Assessing the environmental impact and payback of carbon nanotube supported CO2 capture technologies using LCA methodology. 8 Journal of Cleaner Production 2020; 270: 122465.

[86] NREL, Energy and Carbon Payback Times for Modern US Utility Photovoltaic Systems, National Renewable Energy Lab.(NREL), Golden, CO,United States, 2024.

[87] D'Agostino D, Mazzarella L. What is a Nearly zero energy building? Overview, implementation and comparison of definitions. Journal of Building Engineering 9 2019; 21: 200-212.

[88] D'Agostino D, Tzeiranaki ST, Zangheri P, Bertoldi P. Assessing nearly zero energy buildings (NZEBs) development in Europe. Energy Strategy Reviews 2021; 36: 100680.

[89] Lagarde Q, Beillard B, Mazen S, Denis MS, Leylavergne J. Performance ratio of photovoltaic installations in France: Comparison between inverters and micro-inverters. Journal of King Saud University-Engineering Sciences 2023; 35(8): 531-538.

[90] Cubukcu M, Gumus H. Performance analysis of a grid-connected photovoltaic plant in eastern Turkey. Sustainable Energy Technologies and Assessments 10 2020; 39: 100724.

[91] Eke R, Demircan H. Performance analysis of a multi crystalline Si photovoltaic module under Mugla climatic conditions in Turkey. Energy conversion and Management 11 2013; 65: 580-586.

[92] Duman AC, Güler Ö. Economic analysis of grid-connected residential rooftop PV systems in Turkey. Renewable Energy 2020; 148: 697-711.

[93] Accessed on the date of: 01.05.2024; Available from: https://www.renewableenergyhub.co.uk/main/solar-panels/solar-panels-carbon-analysis.